System size dependence of the hadronic rescattering effect at energies available at the CERN Large Hadron Collider

Acharya, S.; Adamová, D.; Aglieri Rinella, G.; Agnello, M.; Agrawal, N.; Ahammed, Z.; Ahmad, S.; Ahn, S. U.; Ahuja, I.; Akindinov, A.; Al-Turany, M.; Aleksandrov, D.; Alessandro, B.; Alfanda, H. M.; Alfaro Molina, R.; Ali, B.; Alici, A.; Alizadehvandchali, N.; Alkin, A.; Alme, J.; Alocco, G.; Alt, T.; Altamura, A. R.; Altsybeev, I.; Alvarado, J. R.; Anaam, M. N.; Andrei, C.; Andreou, N.; Andronic, A.; Anguelov, V.; Antinori, F.; Antonioli, P.; Apadula, N.; Aphecetche, L.; Appelshäuser, H.; Arata, C.; Arcelli, S.; Aresti, M.; Arnaldi, R.; Arneiro, J. G. M. C. A.; Arsene, I. C.; Arslandok, M.; Augustinus, A.; Averbeck, R.; Azmi, M. D.; Baba, H.; Badalà, A.; Bae, J.; Baek, Y. W.; Bai, X.; Bailhache, R.; Bailung, Y.; Balbino, A.; Baldisseri, A.; Balis, B.; Banerjee, D.; Banoo, Z.; Barbera, R.; Barile, F.; Barioglio, L.; Barlou, M.; Barman, B.; Barnaföldi, G. G.; Barnby, L. S.; Barret, V.; Barreto, L.; Bartels, C.; Barth, K.; Bartsch, E.; Bastid, N.; Basu, S.; Batigne, G.; Battistini, D.; Batyunya, B.; Bauri, D.; Bazo Alba, J. L.; Bearden, I. G.; Beattie, C.; Becht, P.; Behera, D.; Belikov, I.; Bell Hechavarria, A. D. C.; Bellini, F.; Bellwied, R.; Belokurova, S.; Beltran, Y. A. V.; Bencedi, G.; Beole, S.; Berdnikov, Y.; Berdnikova, A.; Bergmann, L.; Besoiu, M. G.; Betev, L.; Bhaduri, P. P.; Bhasin, A.; Bhat, M. A.; Bhattacharjee, B.; Bianchi, L.; Bianchi, N.; Bielík, J.; Bielíková, J.; Biernat, J.; Bigot, A. P.; Bilandzic, A.; Biro, G.; Biswas, S.; Bize, N.; Blair, J. T.; Blau, D.; Blidaru, M. B.; Bluhme, N.; Blume, C.; Boca, G.; Bock, F.; Bodova, T.; Bogdanov, A.; Boi, S.; Bok, J.; Boldizsár, L.; Bombara, M.; Bond, P. M.; Bonomi, G.; Borel, H.; Borissov, A.; Borquez Carcamo, A. G.; Bossi, H.; Botta, E.; Bouziani, Y. E. M.; Bratrud, L.; Braun-Munzinger, P.; Bregant, M.; Broz, M.; Bruno, G. E.; Buckland, M. D.; Budnikov, D.; Buesching, H.; Bufalino, S.; Buhler, P.; Burmasov, N.; Buthelezi, Z.; Bylinkin, A.; Bysiak, S. A.; Cai, M.; Caines, H.; Caliva, A.; Calvo Villar, E.; Camacho, J. M. M.; Camerini, P.; Canedo, F. D. M.; Cantway, S. L.; Carabas, M.; Carballo, A. A.; Carnesecchi, F.; Caron, R.; Carvalho, L. A. D.; Castillo Castellanos, J.; Catalano, F.; Ceballos Sanchez, C.; Chakaberia, I.; Chakraborty, P.; Chandra, S.; Chapeland, S.; Chartier, M.; Chattopadhyay, S.; Chattopadhyay, S.; Cheng, T.; Cheshkov, C.; Cheynis, B.; Chibante Barroso, V.; Chinellato, D. D.; Chizzali, E. S.; Cho, J.; Cho, S.; Chochula, P.; Choudhury, D.; Christakoglou, P.; Christensen, C. H.; Christiansen, P.; Chujo, T.; Ciacco, M.; Cicalo, C.; Cindolo, F.; Ciupek, M. R.; Clai, G.; Colamaria, F.; Colburn, J. S.; Colella, D.; Colocci, M.; Concas, M.; Conesa Balbastre, G.; Conesa Del Valle, Z.; Contin, G.; Contreras, J. G.; Coquet, M. L.; Cortese, P.; Cosentino, M. R.; Costa, F.; Costanza, S.; Cot, C.; Crkovská, J.; Crochet, P.; Cruz-Torres, R.; Cui, P.; Dainese, A.; Danisch, M. C.; Danu, A.; Das, P.; Das, P.; Das, S.; Dash, A. R.; Dash, S.; de Caro, A.; de Cataldo, G.; de Cuveland, J.; de Falco, A.; de Gruttola, D.; De Marco, N.; de Martin, C.; de Pasquale, S.; Deb, R.; Del Grande, R.; Dello Stritto, L.; Deng, W.; Dhankher, P.; di Bari, D.; di Mauro, A.; Diab, B.; Diaz, R. A.; Dietel, T.; Ding, Y.; Ditzel, J.; Divià, R.; Dixit, D. U.; Djuvsland, Ø.; Dmitrieva, U.; Dobrin, A.; Dönigus, B.; Dubinski, J. M.; Dubla, A.; Dudi, S.; Dupieux, P.; Durkac, M.; Dzalaiova, N.; Eder, T. M.; Ehlers, R. J.; Eisenhut, F.; Ejima, R.; Elia, D.; Erazmus, B.; Ercolessi, F.; Espagnon, B.; Eulisse, G.; Evans, D.; Evdokimov, S.; Fabbietti, L.; Faggin, M.; Faivre, J.; Fan, F.; Fan, W.; Fantoni, A.; Fasel, M.; Fecchio, P.; Feliciello, A.; Feofilov, G.; Fernández Téllez, A.; Ferrandi, L.; Ferrer, M. B.; Ferrero, A.; Ferrero, C.; Ferretti, A.; Feuillard, V. J. G.; Filova, V.; Finogeev, D.; Fionda, F. M.; Flatland, E.; Flor, F.; Flores, A. N.; Foertsch, S.; Fokin, I.; Fokin, S.; Fragiacomo, E.; Frajna, E.; Fuchs, U.; Funicello, N.; Furget, C.; Furs, A.; Fusayasu, T.; Gaardhøje, J. J.; Gagliardi, M.; Gago, A. M.; Gahlaut, T.; Galvan, C. D.; Gangadharan, D. R.; Ganoti, P.; Garabatos, C.; García Chávez, T.; Garcia-Solis, E.; Gargiulo, C.; Gasik, P.; Gautam, A.; Gay Ducati, M. B.; Germain, M.; Ghimouz, A.; Ghosh, C.; Giacalone, M.; Gioachin, G.; Giubellino, P.; Giubilato, P.; Glaenzer, A. M. C.; Glässel, P.; Glimos, E.; Goh, D. J. Q.; Gonzalez, V.; Gorgon, M.; Goswami, K.; Gotovac, S.; Grabski, V.;

Published
DOI:10.1103/PhysRevC.109.014911

Graczykowski, L. K.; Grecka, E.; Grelli, A.; Grigoras, C.; Grigoriev, V.; Grigoryan, S.; Grosa, F.; Grosse-Oetringhaus, J. F.; Grosso, R.; Grund, D.; Grunwald, N. A.; Guardiano, G. G.; Guernane, R.; Guilbaud, M.; Gulbrandsen, K.; Gündem, T.; Gunji, T.; Guo, W.; Gupta, A.; Gupta, R.; Gupta, R.; Gwizdziel, K.; Gyulai, L.; Hadjidakis, C.; Haider, F. U.; Haidlova, S.; Hamagaki, H.; Hamdi, A.; Han, Y.; Hanley, B. G.; Hannigan, R.; Hansen, J.; Haque, M. R.; Harris, J. W.; Harton, A.; Hassan, H.; Hatzifotiadou, D.; Hauer, P.; Havener, L. B.; Heckel, S. T.; Hellbär, E.; Helstrup, H.; Hemmer, M.; Herman, T.; Herrera Corral, G.; Herrmann, F.; Herrmann, S.; Hetland, K. F.; Heybeck, B.; Hillemanns, H.; Hippolyte, B.; Hoffmann, F. W.; Hofman, B.; Hong, G. H.; Horst, M.; Horzyk, A.; Hou, Y.; Hristov, P.; Hughes, C.; Huhn, P.; Huhta, L. M.; Humanic, T. J.; Hutson, A.; Hutter, D.; Ilkaev, R.; Ilyas, H.; Inaba, M.; Innocenti, G. M.; Ippolitov, M.; Isakov, A.; Isidori, T.; Islam, M. S.; Ivanov, M.; Ivanov, M.; Ivanov, V.; Iversen, K. E.; Jablonski, M.; Jacak, B.; Jacazio, N.; Jacobs, P. M.; Jadlovska, S.; Jadlovsky, J.; Jaelani, S.; Jahnke, C.; Jakubowska, M. J.; Janik, M. A.; Janson, T.; Ji, S.; Jia, S.; Jimenez, A. A. P.; Jonas, F.; Jones, D. M.; Jowett, J. M.; Jung, J.; Jung, M.; Junique, A.; Jusko, A.; Kabus, M. J.; Kaewjai, J.; Kalinak, P.; Kalteyer, A. S.; Kalweit, A.; Kaplin, V.; Karasu Uysal, A.; Karatovic, D.; Karavichev, O.; Karavicheva, T.; Karczmarczyk, P.; Karpechev, E.; Kebschull, U.; Keidel, R.; Keijdener, D. L. D.; Keil, M.; Ketzer, B.; Khade, S. S.; Khan, A. M.; Khan, S.; Khanzadeev, A.; Kharlov, Y.; Khatun, A.; Khuntia, A.; Kileng, B.; Kim, B.; Kim, C.; Kim, D. J.; Kim, E. J.; Kim, J.; Kim, J. S.; Kim, J.; Kim, J.; Kim, M.; Kim, S.; Kim, T.; Kimura, K.; Kirsch, S.; Kisel, I.; Kiselev, S.; Kisiel, A.; Kitowski, J. P.; Klay, J. L.; Klein, J.; Klein, S.; Klein-Bösing, C.; Kleiner, M.; Klemenz, T.; Kluge, A.; Knospe, A. G.; Kobdaj, C.; Kollegger, T.; Kondratyev, A.; Kondratyeva, N.; Kondratyuk, E.; Konig, J.; Konigstorfer, S. A.; Konopka, P. J.; Kornakov, G.; Korwieser, M.; Koryciak, S. D.; Kotliarov, A.; Kovalenko, V.; Kowalski, M.; Kozhuharov, V.; Králik, I.; Kraváková, A.; Krcal, L.; Krivda, M.; Krizek, F.; Krizkova Gajdosova, K.; Kroesen, M.; Krüger, M.; Krupova, D. M.; Kryshen, E.; Kuera, V.; Kuhn, C.; Kuijer, P. G.; Kumaoka, T.; Kumar, D.; Kumar, L.; Kumar, N.; Kumar, S.; Kundu, S.; Kurashvili, P.; Kurepin, A.; Kurepin, A. B.; Kuryakin, A.; Kushpil, S.; Kweon, M. J.; Kwon, Y.; La Pointe, S. L.; La Rocca, P.; Lakrathok, A.; Lamanna, M.; Landou, A. R.; Langoy, R.; Larionov, P.; Laudi, E.; Lautner, L.; Lavicka, R.; Lea, R.; Lee, H.; Legrand, I.; Legras, G.; Lehrbach, J.; Lelek, T. M.; Lemmon, R. C.; León Monzón, I.; Lesch, M. M.; Lesser, E. D.; Lévai, P.; Li, X.; Lien, J.; Lietava, R.; Likmeta, I.; Lim, B.; Lim, S. H.; Lindenstruth, V.; Lindner, A.; Lippmann, C.; Liu, D. H.; Liu, J.; Liveraro, G. S. S.; Lofnes, I. M.; Loizides, C.; Lokos, S.; Lömker, J.; Loncar, P.; Lopez, X.; López Torres, E.; Lu, P.; Lugo, F. V.; Luhder, J. R.; Lunardon, M.; Luparello, G.; Ma, Y. G.; Mager, M.; Maire, A.; Majerz, E. M.; Makariev, M. V.; Malaev, M.; Malfattore, G.; Malik, N. M.; Malik, Q. W.; Malik, S. K.; Malinina, L.; Mallick, D.; Mallick, N.; Mandaglio, G.; Mandal, S. K.; Manko, V.; Manso, F.; Manzari, V.; Mao, Y.; Marcjan, R. W.; Margagliotti, G. V.; Margotti, A.; Marín, A.; Markert, C.; Martinengo, P.; Martínez, M. I.; Martínez García, G.; Martins, M. P. P.; Masciocchi, S.; Masera, M.; Masoni, A.; Massacrier, L.; Massen, O.; Mastroserio, A.; Matonoha, O.; Mattiazzo, S.; Matyja, A.; Mayer, C.; Mazuecos, A. L.; Mazzaschi, F.; Mazzilli, M.; Mdhluli, J. E.; Melikyan, Y.; Menchaca-Rocha, A.; Mendez, J. E. M.; Meninno, E.; Menon, A. S.; Meres, M.; Mhlanga, S.; Miake, Y.; Micheletti, L.; Mihaylov, D. L.; Mikhaylov, K.; Mishra, A. N.; Mikowiec, D.; Modak, A.; Mohanty, B.; Mohisin Khan, M.; Molander, M. A.; Monira, S.; Mordasini, C.; Moreira de Godoy, D. A.; Morozov, I.; Morsch, A.; Mrnjavac, T.; Muccifora, V.; Muhuri, S.; Mulligan, J. D.; Mulliri, A.; Munhoz, M. G.; Munzer, R. H.; Murakami, H.; Murray, S.; Musa, L.; Musinsky, J.; Myrcha, J. W.; Naik, B.; Nambrath, A. I.; Nandi, B. K.; Nania, R.; Nappi, E.; Nassirpour, A. F.; Nath, A.; Nattrass, C.; Naydenov, M. N.; Neagu, A.; Negru, A.; Nellen, L.; Nepeivoda, R.; Nese, S.; Neskovic, G.; Nicassio, N.; Nielsen, B. S.; Nielsen, E. G.; Nikolaev, S.; Nikulin, S.; Nikulin, V.; Noferini, F.; Noh, S.; Nomokonov, P.; Norman, J.; Novitzky, N.; Nowakowski, P.; Nyanin, A.; Nystrand, J.; Ogino, M.; Oh, S.; Ohlson, A.; Okorokov, V. A.; Oleniacz, J.; Oliveira da Silva, A. C.; Onnerstad, A.; Oppedisano, C.; Ortiz Velasquez, A.; Otwinowski, J.; Oya, M.; Oyama, K.; Pachmayer, Y.; Padhan, S.; Pagano, D.; Pai, G.; Paisano-Guzmán, S.; Palasciano, A.; Panebianco, S.; Park, H.; Park, H.; Park, J.; Parkkila, J. E.; Patley, Y.; Patra, R. N.; Paul, B.; Pei, H.; Peitzmann, T.; Peng, X.; Pennisi, M.; Perciballi, S.; Peresunko, D.; Perez, G. M.; Pestov, Y.; Petrov, V.; Petrovici, M.; Pezzi, R. P.; Piano, S.; Pikna, M.; Pillot, P.; Pinazza, O.; Pinsky, L.; Pinto, C.; Pisano, S.; Posko, M.; Planinic, M.; Pliquett, F.; Poghosyan, M. G.; Polichtchouk, B.; Politano', S.; Poljak, N.; Pop, A.; Porteboeuf-Houssais, S.; Pozdniakov, V.; Pozos, I. Y.; Pradhan, K. K.; Prasad, S. K.; Prasad, S.; Preghenella, R.; Prino, F.; Pruneau, C. A.; Pshenichnov, I.; Puccio, M.; Pucillo, S.; Pugelova, Z.; Qiu, S.; Quaglia, L.; Ragoni, S.; Rai, A.; Rakotozafindrabe, A.; Ramello, L.; Rami, F.; Rancien, T. A.; Rasa, M.; Räsänen, S. S.; Rath, R.; Rauch, M. P.; Ravasenga, I.; Read, K. F.; Reckziegel, C.; Redelbach, A. R.; Redlich, K.; Reetz, C. A.; Regules-Medel, H. D.; Rehman, A.; Reidt, F.; Reme-Ness, H. A.; Rescakova, Z.; Reygers, K.; Riabov, A.; Riabov, V.; Ricci, R.; Richter, M.; Riedel, A. A.; Riegler, W.; Riffero, A. G.; Ristea, C.; Rodriguez, M. V.; Rodríguez Cahuantzi, M.; Rodríguez Ramírez, S. A.; Røed, K.; Rogalev, R.; Rogochaya, E.; Rogoschinski, T. S.; Rohr, D.; Röhrich, D.; Rojas, P. F.; Rojas Torres, S.; Rokita, P. S.; Romanenko, G.; Ronchetti, F.; Rosano, A.; Rosas, E. D.; Roslon, K.; Rossi, A.; Roy, A.; Roy, S.; Rubini, N.; Ruggiano, D.; Rui, R.; Russek, P. G.; Russo, R.; Rustamov, A.; Ryabinkin, E.; Ryabov, Y.; Rybicki, A.; Rytkonen, H.; Ryu, J.; Rzesa, W.; Saarimaki, O. A. M.; Sadhu, S.; Sadovsky, S.; Saetre, J.; Šafaík, K.; Saha, P.; Saha, S. K.; Saha, S.; Sahoo, B.; Sahoo, B.; Sahoo, R.; Sahoo, S.; Sahu, D.; Sahu, P. K.; Saini, J.; Sajdakova, K.; Sakai, S.; Salvan, M. P.; Sambyal, S.; Samitz, D.; Sanna, I.; Saramela, T. B.; Sarma, P.; Sarritzu, V.; Sarti, V. M.; Sas, M. H. P.; Sawan, S.; Schambach, J.; Scheid, H. S.; Schiaua, C.; Schicker, R.; Schlepper, F.; Schmah, A.; Schmidt, C.; Schmidt, H. R.; Schmidt, M. O.; Schmidt, M.; Schmidt, N. V.; Schmier, A. R.; Schotter, R.; Schröter, A.; Schukraft, J.; Schweda, K.; Scioli, G.; Scomparin, E.; Seger, J. E.; Sekiguchi, Y.; Sekihata, D.; Selina, M.; Selyuzhenkov, I.; Senyukov, S.; Seo, J. J.; Serebryakov, D.; Šerkšnytä--, L.; Sevcenco, A.; Shaba, T. J.; Shabetai, A.; Shahoyan, R.; Shangaraev, A.; Sharma, A.; Sharma, B.; Sharma, D.; Sharma, H.; Sharma, M.; Sharma, S.; Sharma, S.; Sharma, U.; Shatat, A.; Sheibani, O.; Shigaki, K.; Shimomura, M.; Shin, J.; Shirinkin, S.; Shou, Q.; Sibiriak, Y.; Siddhanta, S.; Siemiarczuk, T.; Silva, T. F.; Silvermyr, D.;

Simantathammakul, T.; Simeonov, R.; Singh, B.; Singh, B.; Singh, K.; Singh, R.; Singh, R.; Singh, R.; Singh, S.; Singh, V. K.; Singhal, V.; Sinha, T.; Sitar, B.; Sitta, M.; Skaali, T. B.; Skorodumovs, G.; Slupecki, M.; Smirnov, N.; Snellings, R. J. M.; Solheim, E. H.; Song, J.; Sonnabend, C.; Soramel, F.; Soto-Hernandez, A. B.; Spijkers, R.; Sputowska, I.; Staa, J.; Stachel, J.; Stan, I.; Steffanic, P. J.; Stiefelmaier, S. F.; Stocco, D.; Storehaug, I.; Stratmann, P.; Strazzi, S.; Sturniolo, A.; Stylianidis, C. P.; Suaide, A. A. P.; Suire, C.; Sukhanov, M.; Suljic, M.; Sultanov, R.; Sumberia, V.; Sumowidagdo, S.; Swain, S.; Szarka, I.; Szymkowski, M.; Taghavi, S. F.; Taillepied, G.; Takahashi, J.; Tambave, G. J.; Tang, S.; Tang, Z.; Tapia Takaki, J. D.; Tapus, N.; Tarasovicova, L. A.; Tarzila, M. G.; Tassielli, G. F.; Tauro, A.; Tavira García, A.; Tejeda Muñoz, G.; Telesca, A.; Terlizzi, L.; Terrevoli, C.; Thakur, S.; Thomas, D.; Tikhonov, A.; Tiltmann, N.; Timmins, A. R.; Tkacik, M.; Tkacik, T.; Toia, A.; Tokumoto, R.; Tomohiro, K.; Topilskaya, N.; Toppi, M.; Tork, T.; Torres, P. V.; Torres, V. V.; Torres Ramos, A. G.; Trifiró, A.; Triolo, A. S.; Tripathy, S.; Tripathy, T.; Trogolo, S.; Trubnikov, V.; Trzaska, W. H.; Trzcinski, T. P.; Tumkin, A.; Turrisi, R.; Tveter, T. S.; Ullaland, K.; Ulukutlu, B.; Uras, A.; Usai, G. L.; Vala, M.; Valle, N.; van Doremalen, L. V. R.; van Leeuwen, M.; van Veen, C. A.; van Weelden, R. J. G.; Vande Vyvre, P.; Varga, D.; Varga, Z.; Vasileiou, M.; Vasiliev, A.; Vázquez Doce, O.; Vazquez Rueda, O.; Vechernin, V.; Vercellin, E.; Vergara Limón, S.; Verma, R.; Vermunt, L.; Vértesi, R.; Verweij, M.; Vickovic, L.; Vilakazi, Z.; Villalobos Baillie, O.; Villani, A.; Vinogradov, A.; Virgili, T.; Virta, M. M. O.; Vislavicius, V.; Vodopyanov, A.; Volkel, B.; Völkl, M. A.; Voloshin, K.; Voloshin, S. A.; Volpe, G.; von Haller, B.; Vorobyev, I.; Vozniuk, N.; Vrláková, J.; Wan, J.; Wang, C.; Wang, D.; Wang, Y.; Wang, Y.; Wegrzynek, A.; Weiglhofer, F. T.; Wenzel, S. C.; Wessels, J. P.; Wiechula, J.; Wikne, J.; Wilk, G.; Wilkinson, J.; Willems, G. A.; Windelband, B.; Winn, M.; Wright, J. R.; Wu, W.; Wu, Y.; Xu, R.; Yadav, A.; Yadav, A. K.; Yalcin, S.; Yamaguchi, Y.; Yang, S.; Yano, S.; Yin, Z.; Yoo, I. -K.; Yoon, J. H.; Yu, H.; Yuan, S.; Yuncu, A.; Zaccolo, V.; Zampolli, C.; Zanone, F.; Zardoshti, N.; Zarochentsev, A.; Závada, P.; Zaviyalov, N.; Zhalov, M.; Zhang, B.; Zhang, C.; Zhang, L.; Zhang, S.; Zhang, X.; Zhang, Y.; Zhang, Z.; Zhao, M.; Zherebchevskii, V.; Zhi, Y.; Zhou, D.; Zhou, Y.; Zhu, J.; Zhu, Y.; Zugravel, S. C.; Zurlo, N.. - In: PHYSICAL REVIEW C. - ISSN 2469-9985. - STAMPA. - 109:1(2024), pp. 1-18. [10.1103/PhysRevC.109.014911]

System-size dependence of the hadronic rescattering effect at energies available at the CERN Large Hadron Collider

S. Acharya *et al.*[*]
(ALICE Collaboration)

(Received 22 September 2023; accepted 22 December 2023; published 29 January 2024)

The first measurements of $K^*(892)^0$ resonance production as a function of charged-particle multiplicity in Xe-Xe collisions at $\sqrt{s_{NN}} = 5.44$ TeV and pp collisions at $\sqrt{s} = 5.02$ TeV using the ALICE detector are presented. The resonance is reconstructed at midrapidity ($|y| < 0.5$) using the hadronic decay channel $K^{*0} \to K^{\pm}\pi^{\mp}$. Measurements of transverse-momentum integrated yield, mean transverse-momentum, nuclear modification factor of K^{*0}, and yield ratios of resonance to stable hadron (K^{*0}/K) are compared across different collision systems (pp, p-Pb, Xe-Xe, and Pb-Pb) at similar collision energies to investigate how the production of K^{*0} resonances depends on the size of the system formed in these collisions. The hadronic rescattering effect is found to be independent of the size of colliding systems and mainly driven by the produced charged-particle multiplicity, which is a proxy of the volume of produced matter at the chemical freeze-out. In addition, the production yields of K^{*0} in Xe-Xe collisions are utilized to constrain the dependence of the kinetic freeze-out temperature on the system size using the hadron resonance gas–partial chemical equilibrium model.

DOI: 10.1103/PhysRevC.109.014911

I. INTRODUCTION

Production of hadrons consisting of light-flavored quarks (u, d, and s) have been extensively studied in heavy-ion collisions as well as in small collision systems like pp and p-Pb [1–8] at CERN Large Hadron Collider (LHC) energies to investigate the bulk properties of strongly interacting quantum chromodynamics (QCD) matter of deconfined quarks and gluons, known as the quark-gluon plasma (QGP) [9–23]. The produced QGP is modelled by hydrodynamical equations [24,25]. The system while evolving cools down, and after a certain time, hadronization takes place [26–31]. As the temperature of the system dials down further, it first reaches a space-time surface called chemical freeze-out surface [32] where the hadronic abundances get fixed, and then a kinetic freeze-out (T_{kin}) surface where the hadrons momenta get frozen [33,34]. After the kinetic freeze-out surface, particles stream freely to the detectors. In these collisions, several kinds of light and heavy flavor hadrons and resonances with different flavors of valence quark content, mass, and lifetime are produced. Each of these hadrons and resonances possesses unique characteristic features that can be exploited to study the properties of the medium. Hadron yields are used as an experimental input in the thermal model [35–39] to extract the chemical freeze-out temperature, baryon chemical potential, and volume of the produced matter. The transverse-momentum (p_T) spectra of hadrons are fitted with a hydrodynamics-based model, such as the blast-wave model [40], to obtain the kinetic freeze-out temperature [34,41] and collective radial expansion velocity [41] of the medium. The phase between the chemical and kinetic freeze-out surface is termed as the hadronic phase [42]. Properties of the hadronic phase can be probed by studying short-lived resonance particles which decay via the strong interaction. Short-lived resonances have a lifetime comparable to that of the hadronic phase and, therefore, their decay products get engaged in regeneration [43,44] and rescattering [45,46] processes. These processes depend on the hadronic cross section [47–49] of the decay products of the resonance inside the hadronic medium, the lifetime of the resonance particle, density of the hadron gas, and the hadronic phase lifetime. The presence of these final-state hadronic interactions leads to the modification of experimentally measured yields of resonance particles [50,51].

To probe the final-state hadronic interactions, extensive study for the production of light flavor resonances with different lifetimes (τ), e.g., K^{*0} ($\tau \simeq 4$ fm/c) and $\phi(1020)$ ($\tau \simeq 40$ fm/c) has been carried out previously in various collision systems [6,46,52–67]. The p_T-integrated yield of K^{*0} relative to kaons is found to be suppressed in central heavy-ion collisions compared to pp, peripheral heavy-ion collisions, and to thermal model predictions, whereas no such suppression is observed for the ϕ meson. The observed reduction in measurable yield suggests that the rescattering of K^{*0} decay products in the hadronic phase dominates over regeneration, leading to the suppression of measurable yield. The suppression of K^{*0} meson yields due to the rescattering is dominant at low p_T (<3 GeV/c) from the study of p_T-differential K^{*0}/K yield ratio [45]. Furthermore, at high p_T, the phenomenon of energy loss by energetic partons traversing the dense medium formed

[*]Full author list given at the end of the article.

in high-energy heavy-ion collisions affects the production yield of K^{*0} and ϕ resonances [6,68] compared to the pp collisions. The energy loss process depends on the lifetime of the dense matter, initial medium density, the path length traversed by the parton, and the parton flavor. The modification in the yield of high-p_T particles is quantified using the nuclear modification factor (R_{AA}) [14] defined as

$$R_{AA} = \frac{1}{\langle T_{AA}\rangle}\frac{\mathrm{d}^2N^{AA}/(\mathrm{d}y\mathrm{d}p_T)}{\mathrm{d}^2\sigma^{pp}/(\mathrm{d}y\mathrm{d}p_T)}, \quad (1)$$

where $\mathrm{d}^2N^{\mathrm{AA}}/(\mathrm{d}y\mathrm{d}p_T)$ is the yield of the particle in heavy-ion collisions and σ^{pp} is its production cross section in pp collisions. The average nuclear overlap function is denoted by $\langle T_{AA}\rangle$ and can be estimated as $\langle T_{AA}\rangle = \langle N_{\mathrm{coll}}\rangle/\sigma_{\mathrm{inel}}$, where $\langle N_{\mathrm{coll}}\rangle$ is the average number of binary nucleon–nucleon collisions obtained from Monte Carlo Glauber simulations [69] and σ_{inel} is the inelastic pp cross section [70]. The R_{AA} measurements for K^{*0} and ϕ in Pb-Pb collisions at $\sqrt{s_{NN}} = 2.76$ and 5.02 TeV show that at high p_T (>6 GeV/c) energy loss for π, K, p, K^{*0} and ϕ are consistent within uncertainties. This observation suggests that the partonic energy loss in the QGP medium is independent of the flavor of light quarks (u, d, s) [6,41,68].

Recent measurements of light flavor hadron production in high-multiplicity pp and p-Pb collisions show some characteristics [71–75] which have so far been solely attributed to the medium created in heavy-ion collisions. The systems created in pp, p-Pb, and heavy-ion collisions, can be classified based on the final state average charged-particle pseudorapidity density measured at midrapidity ($\langle \mathrm{d}N_{\mathrm{ch}}/\mathrm{d}\eta\rangle_{|\eta|<0.5}$). In small collision systems, multiplicities range from a few to a few tens of charged particles per unit of pseudorapidity. In contrast, in Pb-Pb collisions, multiplicities of a few thousand charged-particles per unit of rapidity can be produced. Recent studies by the ALICE Collaboration at LHC energies show a smooth evolution of the yield or abundance of different hadron species as a function of $\langle \mathrm{d}N_{\mathrm{ch}}/\mathrm{d}\eta\rangle_{|\eta|<0.5}$ across different collision systems and energies [7,8]. In contrast, the mean transverse-momentum ($\langle p_T\rangle$), which depends on the radial flow, follows a different trend across various colliding systems, rising faster in small collision systems (pp, p-Pb) compared to heavy-ion (Pb-Pb) collisions [8]. One of the primary motivations for studying resonances like K^{*0} and ϕ in high-multiplicity pp and p-Pb collisions is to search for the presence of a hadronic phase with a nonzero lifetime in a small collision system. A hint of suppression of K^{*0} meson production in high-multiplicity pp and p-Pb collisions was previously reported by the ALICE Collaboration [53]. In fact, the suppression of K^{*0}/K yield ratio evolves smoothly as a function of $\langle \mathrm{d}N_{\mathrm{ch}}/\mathrm{d}\eta\rangle_{|\eta|<0.5}$ from low-multiplicity pp collisions to central Pb-Pb collisions across different collision energies.

The measurement of K^{*0} production yield in the collisions of medium-sized nuclei such as Xe-Xe provides a test for validating the picture of the smooth evolution of hadronic rescattering across different colliding systems by bridging the gap between p-Pb and Pb-Pb multiplicities. Using the data sets of pp, p-Pb, Xe-Xe, and Pb-Pb collisions, collected by the ALICE Collaboration at center-of-mass energies per nucleon pair ($\sqrt{s_{NN}}$) of about 5 TeV, a systematic study of system-size dependence of hadronic rescattering is possible. In this article, the first measurements of K^{*0} meson production at midrapidity ($|y| < 0.5$) as a function of $\langle \mathrm{d}N_{\mathrm{ch}}/\mathrm{d}\eta\rangle_{|\eta|<0.5}$ in pp collisions at $\sqrt{s} = 5.02$ TeV and in Xe-Xe collisions at $\sqrt{s_{NN}} = 5.44$ TeV are presented. The measured K^{*0} yield and K^{*0}/K yield ratio in these collisions are compared with the results obtained from p-Pb and Pb-Pb collisions to understand the system-size dependency of K^{*0} production and the hadronic rescattering effect. The yield ratio K^{*0}/K is used to constrain the hadronic phase lifetime across different collision systems. Furthermore, the measured K^{*0} yields in Xe-Xe and Pb-Pb collisions are used as an experimental input in a partial chemical equilibrium (PCE) based thermal model HRG-PCE [76] to constrain the kinetic freeze-out temperature. This is a novel procedure to extract T_{kin} that is independent of assumptions about the flow velocity profile and the freeze-out hypersurface [76]. In addition, the mean values of transverse-momentum ($\langle p_T\rangle$) of K^{*0} in different collision systems are also compared to understand the evolution of radial flow from small collision systems to heavy-ion collisions. Moreover, the R_{AA} of K^{*0} at similar charged-particle multiplicity in Pb − Pb and Xe − Xe collisions are compared to shed light on the system-size dependence of parton energy loss.

The organization of the article is as follows. The ALICE experimental setup, data analysis technique, and sources of systematic uncertainties are described in Secs. II, III, and IV, respectively. Results are shown in Sec. V, and the article is finally summarized in Sec. VI. Since the production of particles and antiparticles are in equal amounts at midrapidity at LHC energies [41], the results for K^{*0} and $\overline{K^{*0}}$ are averaged and denoted as K^{*0} throughout the article unless stated otherwise.

II. EXPERIMENTAL APPARATUS, EVENT AND TRACK SELECTION

The production yield of K^{*0} meson is measured in Xe-Xe and pp collisions at $\sqrt{s_{NN}} = 5.44$ TeV and $\sqrt{s} = 5.02$ TeV, respectively, using the data collected by the ALICE detector at the LHC. The Xe-Xe collision events were collected in the year 2017 with a magnetic field strength $B = 0.2$ T, whereas the pp collision events were collected with $B = 0.5$ T in the year 2015. A full description of the ALICE detector and its performance can be found in [77,78]. Analyzed events are selected using a minimum-bias trigger that requires at least one hit in both forward scintillator detectors V0A ($2.8 < \eta < 5.1$) and V0C ($-3.7 < \eta < -1.7$) [79]. Pileup removal involves analyzing hits in the SPD detector, correlating cluster numbers in the ITS and TPC detectors, identifying multiple vertices with the SPD detector, and utilizing the correlation between the SPD and V0M detectors. Beam-induced background and pileup events are eliminated through an offline event selection process, as described in Refs. [8,77] for pp and [41,80] for Xe-Xe collisions. The results for pp collisions presented in this paper are based on the "INEL > 0" event class, which is a subset of inelastic collisions where at least one charged particle is emitted in the pseudorapidity interval $|\eta| < 1$ [81]. In addition, selected events must have one primary collision vertex which is reconstructed

TABLE I. Analyzed multiplicity classes in pp collisions at $\sqrt{s} = 5.02$ TeV.

V0M (%)	0–1	1–5	5–10	10–20	20–30	30–40	40–50	50–70	70–100
Multiplicity classes	I	II	III	IV	V	VI	VII	VIII	IX

using the two innermost layers of the Inner Tracking System (ITS) [82] and is located within ± 10 cm along the beam axis from the nominal center of the ALICE detector. Measurements for K^{*0} production yields are carried out using 1.44×10^6 and 100×10^6 minimum-bias Xe-Xe and pp collision events. The selected events are categorized into distinct classes based on their centrality in heavy-ion collisions (Xe-Xe) or multiplicity in proton-proton (pp) collisions. These event classes are defined using percentiles of the hadronic cross section. The classification of event classes is accomplished by analyzing the signal deposited in both V0 detectors, referred to as the "V0M amplitude", which is proportional to the charged-particle multiplicity. Various measured observables, such as the transverse momentum (p_T) spectrum, transverse-momentum-integrated yield (dN/dy), mean transverse momentum ($\langle p_T \rangle$), yield ratios of resonances to stable particles, kinetic freeze-out temperature ($T_{\rm kin}$), and nuclear modification factor (R_{AA}), are presented for different multiplicity (or centrality for heavy-ion collisions) classes as a function of pseudorapidity density ($\langle dN_{\rm ch}/d\eta \rangle_{|\eta|<0.5}$) [83,84].

In Xe-Xe collisions, the measurements are conducted in four different centrality classes: 0–30%, 30–50%, 50–70%, and 70–90%. The centrality classes of 0–30% and 70–90%, represent central and peripheral collisions, respectively. On the other hand, in pp collisions, the measurements are performed in nine different multiplicity classes, as listed in Table I, with class I having the highest multiplicity and class IX having the lowest multiplicity.

Charged tracks in a selected event are reconstructed using the ITS [82] and time projection chamber (TPC) [85] detectors, which are located within a solenoid that provides a homogeneous magnetic field. In order to ensure good track quality, a set of track selection criteria are used, as done in previous works [53,86]. Charged tracks coming from the primary collision vertex are selected with minimum p_T of 0.15 GeV/c and $|\eta| < 0.8$. Selected tracks must have at least one hit in the two innermost layers of the ITS and must have crossed a minimum of 70 out of total 159 rows along the transverse readout plane of the TPC. The maximum χ^2 per space point in the TPC and ITS obtained from the track fit are required to be 4 and 36, respectively. To minimize the contribution of secondary charged particles, the distance of closest approach in the transverse plane of reconstructed tracks to the primary vertex (DCA$_{xy}$) is required to be smaller than 7σ, where σ is the DCA$_{xy}$ resolution. The DCA$_{xy}$ resolution is found to be p_T dependent and is parametrized as $\sigma = 0.0105 + 0.0350/(p_T)^{1.1}$. The DCA in the longitudinal direction is required to be smaller than 2 cm. Selected charged particles are further identified via the TPC and the time of flight (TOF) [87] detectors using their specific ionization energy loss dE/dx in the TPC and flight time measured in the TOF. Pions (π) and kaons (K) are identified with the condition that their specific energy loss lies within 2 standard deviations ($\sigma_{\rm TPC}$) (for $p > 0.4$), $4\sigma_{\rm TPC}$ (for $0.3 < p < 0.4$), and $6\sigma_{\rm TPC}$ (for $p < 0.3$) from their expected dE/dx, where $\sigma_{\rm TPC}$ corresponds to the dE/dx resolution (typically $\approx$5% of the measured dE/dx value) of the TPC. Furthermore, if the hit for a track is available in the TOF, the measured time of flight is required to be within 3σ from its expected value for each particle species [88].

III. ANALYSIS DETAILS

The K^{*0} meson being a short-lived resonance is reconstructed using the invariant mass method [5] via its hadronic decay channel, $K^*(892)^0 \to K^{\pm}\pi^{\mp}$ with a branching ratio (BR) of 66% [89] for $|y| < 0.5$.

Oppositely charged kaons and pions are paired in the same event to reconstruct the resonance signal. The resulting invariant-mass distribution of unlike sign charge $K\pi$ pair consists of a signal with significant combinatorial background, which is estimated using the mixed-event method [53] (for $0.4 < p_T < 0.8$ GeV/c in Xe-Xe collisions like-sign pairs from the same event [53] are used to get better description of the combinatorial background). The mixed-event invariant mass distribution is constructed by combining kaons from one event with oppositely charged pions from five other events. Only the events with a similar topology, such as an absolute difference in the z coordinate of their collision vertex less than 1 cm and the centrality difference (for Xe-Xe) or multiplicity percentile (for pp) difference less than 5% are mixed. The mixed-event background is scaled to match the unlike-sign foreground distribution in the invariant mass range 1.1–1.15 GeV/c^2. The left panel of Fig. 1 shows the invariant-mass distribution of unlike charged πK pairs from the same-event along with the rescaled mixed-event background. The unlike sign πK invariant mass distribution with mixed-event background subtracted is shown in the right panel of Fig. 1. The combinatorial background subtracted invariant mass distribution consists of K^{*0} signal and a residual background of correlated pairs. The correlated background pairs can originate from sources such as jets, decays of resonances with misidentified daughters, and decays with multiple daughters. The combinatorial background subtracted invariant mass distribution is fitted with a combination of a nonrelativistic Breit-Wigner distribution and a polynomial of second order. The Breit-Wigner distribution describes the signal of K^{*0}, whereas the residual background is modelled using the polynomial function. The width of K^{*0} is kept fixed to its vacuum value in the fit procedure to estimate the signal, whereas it is allowed to vary freely to estimate the systematic uncertainty. Finally, raw yields of K^{*0} in each p_T interval and event class is obtained from the integral of the Breit-Wigner distribution as done in Refs. [45,68].

The extracted raw yields ($N^{\rm raw}$) are further corrected for detector acceptance and reconstruction efficiency ($A \times \epsilon_{\rm rec}$)

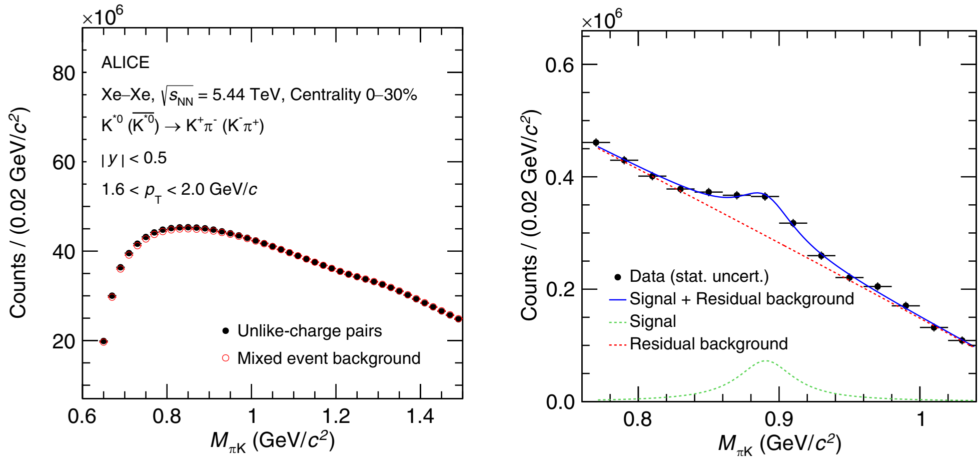

FIG. 1. The left panel shows the invariant mass distribution of unlike sign πK pairs from the same and mixed events. The right panel shows the same but after the mixed-event background subtraction. The mixed event background subtracted invariant mass distribution is fitted with a combination of Breit-Wigner function [5] and second order polynomial distribution. The Breit-Wigner distribution represents the K^{*0} signal and the second order polynomial describes the residual background.

and BR of the decay channel. The $A \times \epsilon_{\rm rec}$ is estimated using dedicated Monte Carlo (MC) event generators, PYTHIA8 [90] for pp collisions and HIJING [91] for Xe-Xe collisions, with particles propagated through a simulation of the ALICE detector using GEANT3 [92]. A weighting procedure of the $A \times \epsilon_{\rm rec}$ is further used to account for the variation of $A \times \epsilon_{\rm rec}$ over the width of a p_T interval in the measured spectrum and for the mismatch in the shape of the spectrum in data and MC simulation [6]. The input p_T distribution in MC is adjusted to match the real distribution using p_T-dependent weights. These are defined as the ratio between the measured p_T distribution after all corrections are applied and the default distribution in MC. In the first iteration, an appropriate fit function with parameters taken from similar analyses is used to parametrize the p_T shape. After all corrections, the p_T spectrum is fitted with the fit function again and the updated parameters are used to modify the weights in the next iteration. Such an iterative procedure is repeated until convergence. Finally, the yields are normalized by the number of accepted events ($N^{\rm acc}_{\rm event}$) to obtain the corrected p_T spectrum in different event classes. Measurements in pp collisions are further corrected for the event loss and the signal loss, evaluated from the MC simulation. The signal loss correction ($f_{\rm SL}$) for K^{*0} is calculated for each multiplicity class by taking the ratio of the simulated K^{*0} p_T spectrum before trigger and event selection with the corresponding p_T spectra after applying all the selections. The $f_{\rm SL}$ is dominant at low p_T in 70–100% multiplicity class with the maximum value of 22%. The event loss correction ($f_{\rm ev}$) corresponds to the fraction of INEL > 0 events that do not pass the event-selection criteria and is estimated in [8]. The $f_{\rm ev}$ is not particle and p_T dependent, and its value spans from 0.99 in 0–1% multiplicity class to 0.71 in 70–100% multiplicity class. The corrected p_T spectrum can be expressed as

$$\frac{1}{N_{\rm event}}\frac{{\rm d}^2N}{{\rm d}y{\rm d}p_T} = \frac{1}{N^{\rm acc}_{\rm event}}\frac{{\rm d}^2N^{\rm raw}}{{\rm d}y{\rm d}p_T}\frac{f_{\rm ev}f_{\rm SL}}{({\rm A}\times\epsilon_{\rm rec}){\rm BR}}. \quad (2)$$

IV. SYSTEMATIC UNCERTAINTIES

Systematic uncertainties on the measured K^{*0} yields originate from various sources, including the signal extraction method, track selection, and particle identification criteria, the method used to match track segments in the ITS with tracks in the TPC, as well as uncertainties in the material budget and interaction cross section. The resulting changes in the K^{*0} yields for each p_T and multiplicity (centrality) interval, obtained from repeating the full analysis chain with the variations and corrections described below, are incorporated as systematic uncertainties. Table II provides a summary of the systematic uncertainties on the measured K^{*0} yields. The reported uncertainties in the table are averaged over all centrality/multiplicity classes and presented for a low- and high-p_T interval.

To evaluate the signal extraction uncertainty, several factors are varied, such as fitting ranges, mixed-event background rescaling region, residual background fit functions, and yield extraction methods. The default case involved fixed-width fits to the invariant mass distributions, based on the background shape. To assess the systematic uncertainty, the boundaries of the fitting ranges are adjusted by 20 MeV/c^2 on both sides. The rescaling of the mixed-event background distribution is shifted to different ranges to examine its impact. The residual background is modeled using a third-order polynomial to study systematic effects. For the primary track selection, the criteria are varied following the procedure described in Ref. [53]. Uncertainties associated with the identification of primary daughter tracks are estimated by varying the selection criteria in the TPC and TOF. Furthermore, uncertainties related to the material budget and hadronic cross section are obtained from Ref. [53]. The total uncertainty, obtained by summing the uncertainties from each source in quadrature, is averaged over all multiplicity classes. In pp collisions, the total uncertainty ranges from 6.5% to 12.3%, while in Xe-Xe collisions, it ranges from 15% to 18%.

TABLE II. Systematic uncertainties on measured K^{*0} yield in pp and Xe-Xe collisions at $\sqrt{s} = 5.02$ TeV and $\sqrt{s_{NN}} = 5.44$ TeV respectively. The systematic uncertainties are shown for different sources for a low- and a high-p_T interval.

	pp [p_{T} (GeV/c)]		Xe-Xe [p_T (GeV/c)]	
Systematic variation	0–0.4	10.0–14.0	0.4–0.8	8.0–12.0
Signal extraction (%)	7.4	9.6	12.7	11.5
Primary track selection (%)	1.9	5.0	7.2	7.1
Particle identification (%)	1.4	5.5	7.1	7.8
ITS–TPC matching (%)	2	negl.	6.4	8.6
Material budget (%)	1.8	negl.	1.4	negl.
Hadronic interaction (%)	2.6	negl.	2.3	negl.
Total (%)	8.7	12.3	17.6	17.8

V. RESULTS

The K^{*0} p_T spectra in pp collisions at $\sqrt{s} = 5.02$ TeV for different multiplicity classes after all corrections mentioned in Sec. III are shown in the upper panel of Fig. 2. The lower panel of Fig. 2 shows the ratios of the K^{*0} p_T spectra in different multiplicity classes to the corresponding spectrum in multiplicity integrated (INEL > 0) pp collisions. An increase in the inverse slopes of the p_T spectra from low to high multiplicity is clearly visible for p_T <4 GeV/c. However, at higher p_T, the spectra in different multiplicity classes have the same shape, indicating that the low p_T processes are primarily responsible for the change in the shape of the p_T spectra from low to high multiplicity classes. The corrected p_T distributions for K^{*0} in four different centrality classes of Xe-Xe collisions at $\sqrt{s_{NN}} = 5.44$ TeV are shown in the left panel of Fig. 3. The right panel of Fig. 3 shows the comparison

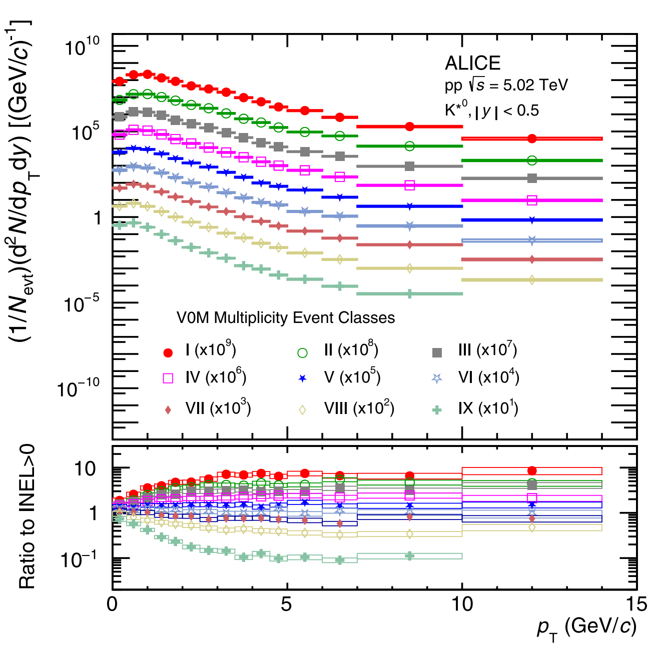

FIG. 2. Upper panel: The p_T spectra of K^{*0} in various multiplicity classes of pp collisions at $\sqrt{s} = 5.02$ TeV. Lower panel: The ratios of the multiplicity-dependent p_T spectra to the multiplicity-integrated INEL > 0 spectra. The statistical and systematic uncertainties are shown as bars and boxes, respectively.

of the K^{*0} p_T spectrum between Xe-Xe and Pb-Pb collisions with similar final-state charged-particle multiplicity. At similar multiplicity values, the K^{*0} p_T distributions in Xe-Xe and Pb-Pb collisions are consistent within uncertainties. The final-state charged-particle multiplicity is a proxy of the volume of the produced matter. It is similar in the central collision of medium (Xe) and mid-central collisions of large (Pb) size nuclei. This indicates that the physics processes such as hadronic rescattering and radial flow, which determine the shape of the p_T distribution in heavy-ion collisions, have a similar effect on the K^{*0} p_T spectra irrespective of the size of the colliding nuclei. The transverse momentum integrated K^{*0} yield $\mathrm{d}N/\mathrm{d}y$ and average transverse momentum $\langle p_T \rangle$ are extracted from the measured p_T spectrum and the extrapolation to the unmeasured regions using a blast-wave function [6]. In pp collisions, K^{*0} is measured down to $p_T = 0$ GeV/c. Therefore, no low-p_T extrapolation is used to extract the $\mathrm{d}N/\mathrm{d}y$ and $\langle p_T \rangle$ in pp collisions. The contribution of the extrapolation on the extracted $\mathrm{d}N/\mathrm{d}y$ is ≈9% (≈13%) in central (peripheral) Xe-Xe collisions. The systematic uncertainties on the extracted $\mathrm{d}N/\mathrm{d}y$, and $\langle p_T \rangle$ are estimated by varying the data points randomly up and down within their systematic uncertainty to obtain the softest and hardest spectra. An additional systematic uncertainty due to the extrapolation of p_T spectra to $p_T = 0$ GeV/c is evaluated in Xe-Xe collisions by using different fit functions (Levy-Tsallis, Boltzmann) for the extrapolation [93,94]. The systematic uncertainty for the extrapolation is ≈2% and ≈1.7% on $\mathrm{d}N/\mathrm{d}y$ and $\langle p_T \rangle$, respectively.

Figure 4 shows the $\mathrm{d}N/\mathrm{d}y$ (left panel) and $\langle p_T \rangle$ (right panel) of K^{*0} as a function of $\langle \mathrm{d}N_{\mathrm{ch}}/\mathrm{d}\eta \rangle^{1/3}_{|\eta|<0.5}$ in pp collisions at $\sqrt{s} = 5.02$ TeV and in Xe-Xe collisions at $\sqrt{s_{NN}} = 5.44$ TeV, where $\langle \mathrm{d}N_{\mathrm{ch}}/\mathrm{d}\eta \rangle^{1/3}_{|\eta|<0.5}$ is proportional to the linear (radial) path through the produced matter. Measurements are compared with the results obtained in p-Pb [5] and Pb-Pb collisions [6] at $\sqrt{s_{NN}} = 5.02$ TeV. A smooth evolution of the $\mathrm{d}N/\mathrm{d}y$ as a function of $\langle \mathrm{d}N_{\mathrm{ch}}/\mathrm{d}\eta \rangle^{1/3}_{|\eta|<0.5}$ is observed across all the collision systems. This suggests that K^{*0} production is solely driven by final-state charged-particle multiplicity, which is used as a proxy for the system size [95]. The $\langle p_T \rangle$ of K^{*0} increases with $\langle \mathrm{d}N_{\mathrm{ch}}/\mathrm{d}\eta \rangle^{1/3}_{|\eta|<0.5}$ for all collision systems, indicating the increase of radial flow velocity from the low-multiplicity event class to the high-multiplicity event class. In contrast to the $\mathrm{d}N/\mathrm{d}y$, intensive variable $\langle p_T \rangle$ shows a strong dependency on the colliding system and does not scale with

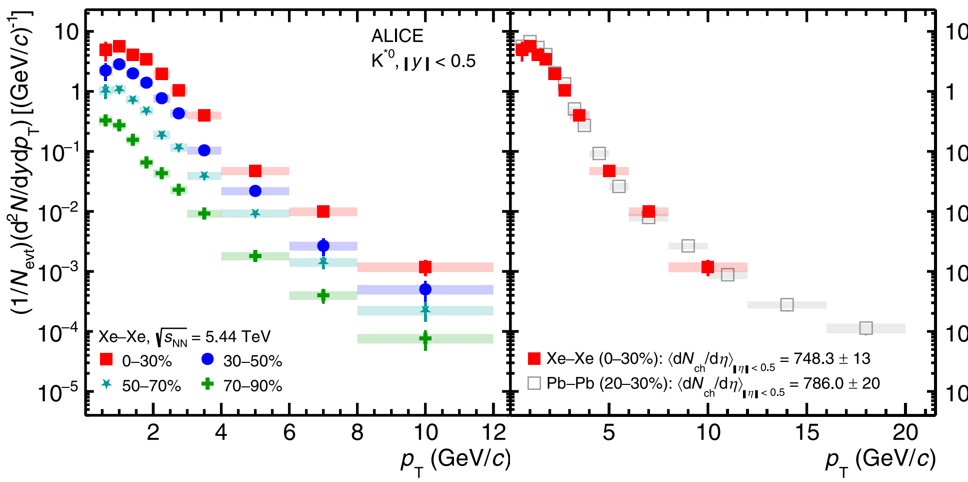

FIG. 3. The left panel shows the p_T distributions of K^{*0} meson in four different centrality classes of Xe-Xe collisions at $\sqrt{s_{NN}} = 5.44$ TeV. The right panel shows the comparison between the K^{*0} p_T spectrum in 0–30% Xe-Xe collisions at $\sqrt{s_{NN}} = 5.44$ TeV and in 20–30% Pb-Pb [6] collisions at $\sqrt{s_{NN}} = 5.02$ TeV, both having similar multiplicities. The statistical and systematic uncertainties are shown by bars and boxes, respectively.

charged-particle multiplicity across all collision systems. The $\langle p_T\rangle$ of K^{*0} increases more steeply in small collision systems compared to heavy-ion collisions. For $\langle dN_{ch}/d\eta\rangle^{1/3}_{|\eta|<0.5}$ >2 the following ordering of $\langle p_T\rangle$ is observed for a fixed multiplicity: $\langle p_T\rangle$ (pp) > $\langle p_T\rangle$ (p–Pb) > $\langle p_T\rangle$ (Xe-Xe) ∼ $\langle p_T\rangle$ (Pb-Pb). In the blast wave fit, where the fit parameters are interpreted in terms of a collective expansion, it is observed that small collision systems exhibit a larger pressure gradient and faster expansion of produced matter compared to heavy-ion collisions with similar charged-particle multiplicity [96,97]. Furthermore, the $\langle p_T\rangle$ of K^{*0} in Xe-Xe and Pb-Pb collisions are comparable at similar $\langle dN_{ch}/d\eta\rangle^{1/3}_{|\eta|<0.5}$, suggesting similar dynamical evolution of the system produced in the collision of large and medium size nuclei at LHC energy. The left panel of Fig. 5 shows the p_T-integrated K^{*0}/K yield ratio as a function of $\langle dN_{ch}/d\eta\rangle^{1/3}_{|\eta|<0.5}$. Measurements in Xe-Xe collisions are compared with the yield ratios obtained in *pp*, *p*-Pb [5], and Pb–Pb [6] collisions at $\sqrt{s_{NN}} = 5.02$ TeV. The kaon yields in *pp* collisions at $\sqrt{s} = 5.02$ TeV are obtained through an extrapolation of kaon yields from *pp* collisions at $\sqrt{s} = 13$ TeV [96] and $\sqrt{s} = 7$ TeV [7]. To perform this extrapolation, the yields at both $\sqrt{s} = 13$ and $\sqrt{s} = 7$ TeV are fitted as a function of $\langle dN_{ch}/d\eta\rangle^{1/3}_{|\eta|<0.5}$ with a first-order polynomial. The resulting fit function value is then used to estimate the kaon yields at the corresponding $\langle dN_{ch}/d\eta\rangle^{1/3}_{|\eta|<0.5}$ for $\sqrt{s} = 5.02$ TeV. To assess the uncertainty in the yield estimation, a Gaussian distribution is constructed for each data point. The mean of the distribution corresponds to the value of the data point, while the standard deviation (σ) represents the associated statistical or systematic uncertainty. For each

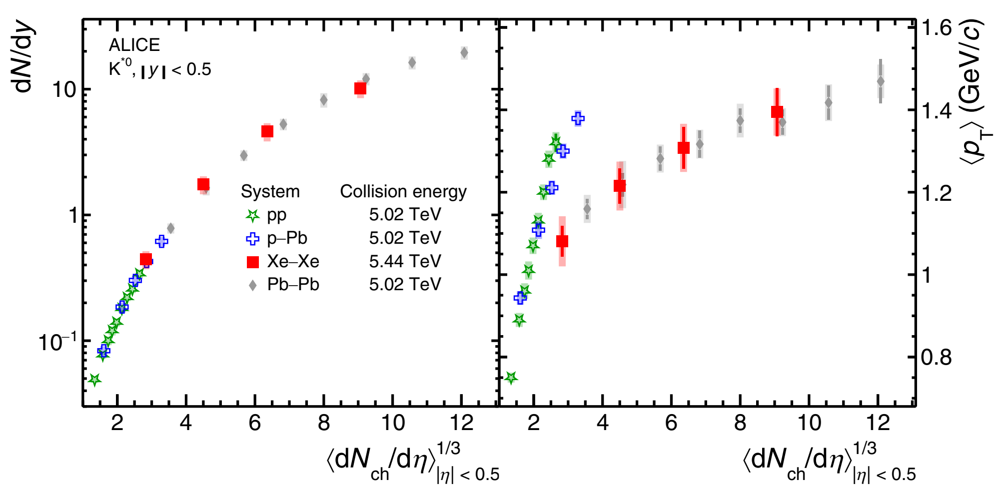

FIG. 4. The dN/dy (left panel) and $\langle p_T\rangle$ (right panel) of K^{*0} as a function of $\langle dN_{ch}/d\eta\rangle^{1/3}_{|\eta|<0.5}$ in *pp* collision at $\sqrt{s} = 5.02$ TeV and in Xe-Xe collisions at $\sqrt{s_{NN}} = 5.44$ TeV. Measurements are compared with the results obtained in *p*-Pb [5] and Pb-Pb [6] collisions at $\sqrt{s_{NN}} =$ 5.02 TeV. Bars and shaded boxes correspond to the statistical and systematic uncertainties, respectively.

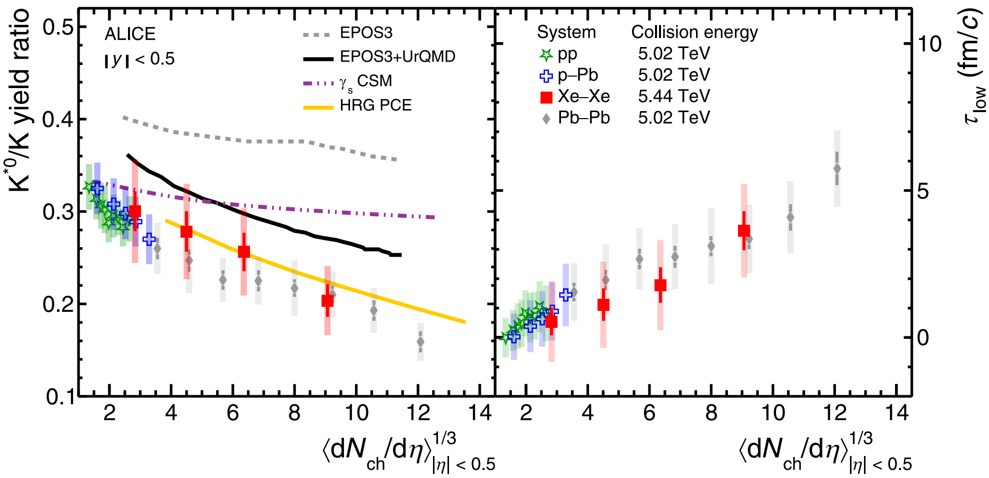

FIG. 5. The left panel shows the measured K^{*0}/K yield ratio along with model calculation. The right panel shows the lower limit of hadronic phase lifetime as a function of $\langle dN_{\rm ch}/d\eta\rangle^{1/3}_{|\eta|<0.5}$ in different collision systems. Bars and shaded boxes represent the statistical and systematic uncertainties, respectively.

data point, a random value is sampled from its corresponding Gaussian distribution. It is assumed that the data points are uncorrelated with multiplicity. A linear fit is then applied to these randomly sampled values. This process is repeated thousands of times, generating multiple linear fits. The standard deviation of the fitting values obtained from these repetitions is considered as the uncertainty of the yield for a given multiplicity. The K^{*0}/K yield ratio in different collision systems shows a smooth evolution with $\langle dN_{\rm ch}/d\eta\rangle^{1/3}_{|\eta|<0.5}$, and is independent of the collision system at similar final-state charged-particle multiplicity. This further confirms the smooth evolution of hadron chemistry, observed for other light flavour hadrons [86]. The K^{*0}/K yield ratio decreases with increasing event multiplicity. This decrease in the K^{*0}/K yield ratio can be understood as the rescattering of K^{*0} meson's decay daughters inside the hadronic phase [45]. Since the lifetime of K^{*0} is comparable to that of the hadronic phase, its decay products scatter in their passage through the hadronic medium changing their momenta and hence affecting the reconstruction of the parent particle, thereby decreasing the measured yield. Measurements in heavy-ion collisions are further compared with the EPOS3 model calculations with and without the hadronic phase [98]. The EPOS3 model calculations are for Pb-Pb collisions at $\sqrt{s_{NN}} = 2.76$ TeV, as no significant quantitative differences are expected between the two energies. In the presence of the hadronic phase, which is modelled by the UrQMD model [99], the EPOS3 generator qualitatively reproduces the multiplicity dependence of the K^{*0}/K yield ratio. The canonical ensemble based statistical model (CSM) [37], which successfully describes the production of other light flavor hadrons in small collision systems and heavy-ion collisions, does not explain the multiplicity dependence of K^{*0}/K yield ratio. The yield ratio is suppressed compared to the γ_s CSM, and the suppression is more prominent in central Xe-Xe and Pb-Pb collisions. In the recent development of the hadron resonance gas (HRG) model, the hadronic phase effect is modelled by a concept of partial chemical equilibrium (PCE) [76]. In this model, decays and regenerations of the resonances obey the law of mass action, ensuring an equilibrium between the abundance of different resonances and their decay products. By applying the HRG-PCE calculation, the measured data points of particle ratios (K^{*0}/K), in heavy-ion collisions can be accurately described. The K^{*0}/K yield ratio can also be used to get an estimate of the lower bound of the hadronic phase lifetime τ, i.e., the time between chemical and kinetic freeze-out. The K^{*0}/K yield ratio at kinetic freeze-out can be expressed as $[K^{*0}/K]_{\rm kinetic} = [K^{*0}/K]_{\rm chemical} \times e^{-\tau/\tau_{K^{*0}}}$, where $\tau_{K^{*0}}$ is the vacuum lifetime of K^{*0}, taken to be 4.16 fm/c. The $[K^{*0}/K]$ yield ratio in the 70–100% multiplicity class of pp collisions at $\sqrt{s} = 5.02$ TeV is used as a proxy for the $[K^{*0}/K]_{\rm chemical}$ and the measured K^{*0}/K yield ratio in different multiplicity or centrality classes of pp, p-Pb, Xe-Xe, and Pb-Pb collisions are used as $[K^{*0}/K]_{\rm kinetic}$. The above procedure estimates the lower bound of the τ with the assumption that there is no regeneration of K^{*0} in the hadronic medium. The hadronic phase lifetime obtained with this simple model is further scaled by a Lorentz factor $\sqrt{1 + (\frac{\langle p_{\rm T}\rangle}{\text{mass of } K^{*0}})^2}$ and the extracted τ values are shown in the right panel of Fig. 5 as a function of $\langle dN_{\rm ch}/d\eta\rangle^{1/3}_{|\eta|<0.5}$. The hadronic phase lifetime evolves smoothly with multiplicity. The lifetime of the hadronic phases produced in Xe-Xe and Pb-Pb collisions are consistent with each other at similar charged-particle multiplicity. The time span by the hadronic phase is reflected in the temperature difference between the chemical and the kinetic freeze-out. The kinetic freeze-out temperature is extracted using the HRG-PCE [76] model fit to the experimentally measured yields of $\pi^{\pm}$, $K^{\pm}$, $p(\overline{p})$, ϕ [6], K^{*0} in 0–30%, 30–50%, and 50–70% centrality classes for Xe-Xe collisions at $\sqrt{s_{NN}} = 5.44$ TeV. The parameters of the fit are the baryon chemical potential, chemical freeze-out temperature, kinetic freeze-out temperature, and freeze-out volume of the system. The baryon chemical potential and chemical freeze-out temperature are fixed at 0 and 155 MeV, respectively, at LHC energies [30,101–103]. Figure 6 shows

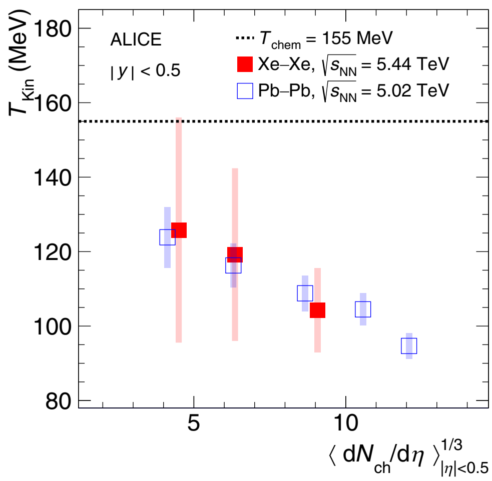

FIG. 6. The kinetic freeze-out temperature estimated using the fit of HRG-PCE model to the measured yields of $\pi^{\pm}$, $K^{\pm}$, $p(\overline{p})$, ϕ, K^{*0} in different centrality classes of Xe-Xe collisions at $\sqrt{s_{NN}} =$ 5.44 TeV. Results are compared with extracted kinetic freeze-out temperature in Pb-Pb collisions at $\sqrt{s_{NN}} = 5.02$ TeV [100].

the kinetic freeze-out temperature obtained from the HRG-PCE fit in Xe-Xe collisions, and the results are compared with the Pb-Pb measurements [100]. The freeze-out temperature is found to increase systematically while moving from central to peripheral centrality class both for Xe-Xe and Pb-Pb collisions due to longer duration of hadronic phase, though the uncertainties are larger in Xe-Xe collisions. The freeze-out temperatures in both collision systems are consistent within uncertainties at similar charged-particle multiplicity. The difference between chemical and kinetic freeze-out temperature supports the presence of a hadronic phase with a finite lifetime in Xe-Xe collisions, a long-lived one in central collisions, and a short-lived one in peripheral collisions. Furthermore, to understand the p_T dependence of the hadronic rescattering effect, the K^{*0}/K yield ratios in Xe-Xe collisions at $\sqrt{s_{NN}} =$ 5.44 TeV are shown in Fig. 7 for two different p_T intervals, $0.4 < p_T < 2.0$ GeV/c and $2.0 < p_T < 4.0$ GeV/c. The results are also compared with the ϕ/K [86] yield ratio. In the low p_T range, the K^{*0}/K yield ratio decreases from peripheral Xe-Xe collisions to central Xe-Xe collisions, whereas ϕ/K remains more or less constant with system size. The observed low p_T suppression of measured K^{*0} yield can be attributed to the rescattering effect of the decay products of K^{*0} in the hadronic phase. The lifetime of ϕ mesons is one order of magnitude larger than that of K^{*0}; therefore, the ϕ meson decay daughters are not expected to be affected by the rescattering in the hadronic phase. As a result, the ϕ/K yield ratio remains constant within uncertainties across the whole range of multiplicities. In contrast to low p_T, at high p_T, both the K^{*0}/K and ϕ/K yield ratios remain flat as a function of $\langle dN_{\rm ch}/d\eta\rangle^{1/3}_{|\eta|<0.5}$. This suggests that the rescattering effect is a low transverse momentum phenomenon.

The left panel of Fig. 8 shows the comparison of the nuclear modification factor R_{AA} of K^{*0} in Xe-Xe and Pb-Pb systems at similar final-state charged-particle multiplicity. The R_{AA} values are found to be less than unity at high p_T in both systems. Similar R_{AA} is observed at both low momentum (hydro-like expansion) and high momentum (partonic energy loss) in Xe-Xe and Pb-Pb collisions at similar charged-particle multiplicity. The centrality dependence of energy loss is studied by measuring the p_T-integrated R_{AA} in the range $4.0 < p_T < 12.0$ GeV/c. The p_T-integrated R_{AA} of K^{*0} as a function of $\langle dN_{\rm ch}/d\eta\rangle^{1/3}_{|\eta|<0.5}$ is shown in the right panel of Fig. 8. Measurements are compared with the results of charged hadrons and are found to be consistent within uncertainties. This suggests that jet quenching does not significantly affect the light-flavor particle species composition for the leading particles. The R_{AA} is smaller in central Xe-Xe collisions compared to the peripheral collisions. This reflects more energy loss via multiple partonic interactions in central collisions, as expected from the longer path length traversed by the hard partons in central collisions.

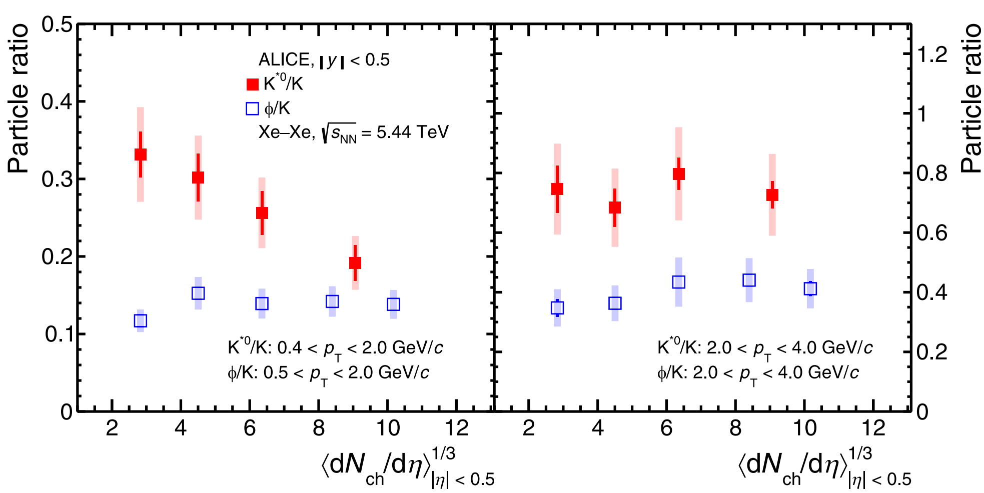

FIG. 7. The K^{*0}/K and ϕ/K yield ratios as a function of $\langle dN_{\rm ch}/d\eta\rangle^{1/3}_{|\eta|<0.5}$ in Xe-Xe collisions at $\sqrt{s_{NN}} = 5.44$ TeV. The left and right panels show the measurements for a low-p_T and a high-p_T interval, respectively. Statistical and systematic uncertainties are represented by bars and shaded boxes.

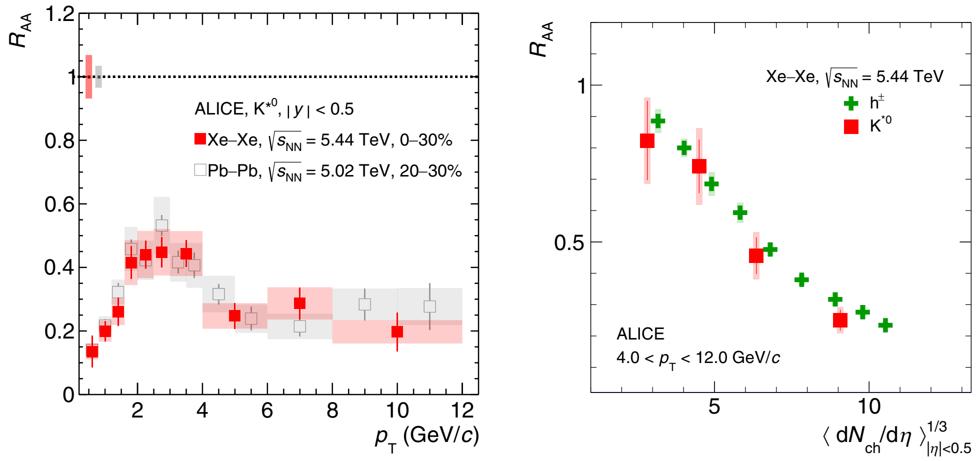

FIG. 8. The left panel shows the nuclear modification factor as a function of p_T for the K^{*0} meson in 0–30 % Xe–Xe collisions at $\sqrt{s_{NN}}$ = 5.44 TeV and in 20–30 % Pb-Pb collisions [6] at $\sqrt{s_{NN}}$ = 5.02 TeV. The right panel shows the R_{AA} of K^{*0} as a function of $\langle dN_{ch}/d\eta\rangle^{1/3}_{|\eta|<0.5}$ for $4.0 < p_T < 12.0$ GeV/c in Xe-Xe collisions. The results are compared to the R_{AA} of charged hadron [80]. Statistical and systematic uncertainties are represented by bars and shaded boxes.

VI. CONCLUSION

The ALICE Collaboration has reported measurements of K^{*0} meson at midrapidity ($|y| < 0.5$) for different centrality and multiplicity classes in Xe-Xe and pp collisions at $\sqrt{s_{NN}}$ = 5.44 TeV and $\sqrt{s}$ = 5.02 TeV, respectively. Both p_T-integrated K^{*0} yield and K^{*0}/K yield ratio are found to smoothly evolve with $\langle dN_{ch}/d\eta\rangle^{1/3}_{|\eta|<0.5}$, independent of the size of the colliding nuclei, confirming a universal scaling of hadron chemistry or relative abundance of hadron species with final-state charged-particle multiplicity at LHC energies. In contrast, the $\langle p_T\rangle$, which depends on the radial expansion velocity of the produced matter, rises more steeply in smaller collision systems compared to the heavy-ion collisions. This indicates that the matter produced in small collision systems expands more rapidly compared to the system produced in heavy-ion collisions. The K^{*0}/K ratio decreases with increasing final-state charged-particle multiplicity. This decrease in the K^{*0}/K yield ratio can be attributed to the rescattering of decay daughters of K^{*0} in the hadronic phase. In addition, the p_T-differential yield ratio K^{*0}/K confirms the dominance of rescattering effect at low p_T. Moreover, the nuclear modification factor for K^{*0} is similar in Xe-Xe and Pb-Pb collisions at similar charged-particle multiplicity indicating a scaling of the parton energy loss with final-state charged-particle multiplicity, independent of the size of the collision system.

The decreasing K^{*0}/K ratio is qualitatively described by the EPOS3 model in presence of hadronic afterburner. The best description of the measurement is provided by the PCE based thermal model, which models the rescattering and the regeneration effect using the law of mass action. In contrast, the canonical ensemble based thermal model does not describe the measured K^{*0}/K yield ratio. Furthermore, the lower limit of hadronic phase lifetime is extracted using K^{*0}/K yield ratios in different colliding systems. A smooth evolution of the lifetime is observed as a function of multiplicity. The kinetic freeze-out temperature is extracted using the HRG-PCE model. A higher temperature is obtained for more peripheral collisions implying an early decoupling of the produced hadrons.

ACKNOWLEDGMENTS

The ALICE Collaboration would like to thank all its engineers and technicians for their invaluable contributions to the construction of the experiment and the CERN accelerator teams for the outstanding performance of the LHC complex. The ALICE Collaboration gratefully acknowledges the resources and support provided by all Grid centres and the Worldwide LHC Computing Grid (WLCG) collaboration. The ALICE Collaboration acknowledges the following funding agencies for their support in building and running the ALICE detector: A. I. Alikhanyan National Science Laboratory (Yerevan Physics Institute) Foundation (ANSL), State Committee of Science and World Federation of Scientists (WFS), Armenia; Austrian Academy of Sciences, Austrian Science Fund (FWF): [M 2467-N36] and Nationalstiftung für Forschung, Technologie und Entwicklung, Austria; Ministry of Communications and High Technologies, National Nuclear Research Center, Azerbaijan; Conselho Nacional de Desenvolvimento Científico e Tecnológico (CNPq), Financiadora de Estudos e Projetos (Finep), Fundação de Amparo à Pesquisa do Estado de São Paulo (FAPESP) and Universidade Federal do Rio Grande do Sul (UFRGS), Brazil; Bulgarian Ministry of Education and Science, within the National Roadmap for Research Infrastructures 2020-2027 (object CERN), Bulgaria; Ministry of Education of China (MOEC), Ministry of Science & Technology of China (MSTC) and National Natural Science Foundation of China (NSFC), China; Ministry of Science and Education and Croatian Science Foundation, Croatia; Centro de Aplicaciones Tecnológicas y Desarrollo Nuclear (CEADEN), Cubaenergía, Cuba; Ministry of Education, Youth and Sports of the Czech Republic, Czech Republic; The Danish Council for Independent Research | Natural Sciences, the VILLUM FONDEN and Danish National Research Foundation (DNRF), Denmark; Helsinki

Institute of Physics (HIP), Finland; Commissariat à l'Energie Atomique (CEA) and Institut National de Physique Nucléaire et de Physique des Particules (IN2P3) and Centre National de la Recherche Scientifique (CNRS), France; Bundesministerium für Bildung und Forschung (BMBF) and GSI Helmholtzzentrum für Schwerionenforschung GmbH, Germany; General Secretariat for Research and Technology, Ministry of Education, Research and Religions, Greece; National Research, Development and Innovation Office, Hungary; Department of Atomic Energy Government of India (DAE), Department of Science and Technology, Government of India (DST), University Grants Commission, Government of India (UGC) and Council of Scientific and Industrial Research (CSIR), India; National Research and Innovation Agency - BRIN, Indonesia; Istituto Nazionale di Fisica Nucleare (INFN), Italy; Japanese Ministry of Education, Culture, Sports, Science and Technology (MEXT) and Japan Society for the Promotion of Science (JSPS) KAKENHI, Japan; Consejo Nacional de Ciencia (CONACYT) y Tecnología, through Fondo de Cooperación Internacional en Ciencia y Tecnología (FONCICYT) and Dirección General de Asuntos del Personal Academico (DGAPA), Mexico; Nederlandse Organisatie voor Wetenschappelijk Onderzoek (NWO), Netherlands; The Research Council of Norway, Norway; Commission on Science and Technology for Sustainable Development in the South (COMSATS), Pakistan; Pontificia Universidad Católica del Perú, Peru; Ministry of Education and Science, National Science Centre and WUT ID-UB, Poland; Korea Institute of Science and Technology Information and National Research Foundation of Korea (NRF), Republic of Korea; Ministry of Education and Scientific Research, Institute of Atomic Physics, Ministry of Research and Innovation and Institute of Atomic Physics and University Politehnica of Bucharest, Romania; Ministry of Education, Science, Research and Sport of the Slovak Republic, Slovakia; National Research Foundation of South Africa, South Africa; Swedish Research Council (VR) and Knut & Alice Wallenberg Foundation (KAW), Sweden; European Organization for Nuclear Research, Switzerland; Suranaree University of Technology (SUT), National Science and Technology Development Agency (NSTDA), Thailand Science Research and Innovation (TSRI) and National Science, Research and Innovation Fund (NSRF), Thailand; Turkish Energy, Nuclear and Mineral Research Agency (TENMAK), Turkey; National Academy of Sciences of Ukraine, Ukraine; Science and Technology Facilities Council (STFC), United Kingdom; National Science Foundation of the United States of America (NSF) and United States Department of Energy, Office of Nuclear Physics (DOE NP), United States of America. In addition, individual groups or members have received support from: European Research Council, Strong 2020 - Horizon 2020 (Grants No. 950692 and No. 824093), European Union; Academy of Finland (Center of Excellence in Quark Matter) (Grants No. 346327 and No. 346328), Finland.

[1] ALICE Collaboration, B. Abelev *et al.*, Multiplicity dependence of pion, kaon, proton and lambda production in p–Pb collisions at $\sqrt{s_{NN}} = 5.02$ TeV, Phys. Lett. B **728**, 25 (2014).

[2] ALICE Collaboration, B. Abelev *et al.*, Centrality dependence of π, K, p production in Pb–Pb collisions at $\sqrt{s_{NN}} = 2.76$ TeV, Phys. Rev. C **88**, 044910 (2013).

[3] ALICE Collaboration, J. Adam *et al.*, Multi-strange baryon production in p–Pb collisions at $\sqrt{s_{\rm NN}} = 5.02$ TeV, Phys. Lett. B **758**, 389 (2016).

[4] ALICE Collaboration, K. Aamodt *et al.*, Production of pions, kaons and protons in pp collisions at $\sqrt{s} = 900$ GeV with ALICE at the LHC, Eur. Phys. J. C **71**, 1655 (2011).

[5] ALICE Collaboration, J. Adam *et al.*, Production of $K^*(892)^0$ and $\phi(1020)$ in p-Pb collisions at $\sqrt{s_{NN}} = 5.02$ TeV, Eur. Phys. J. C **76**, 245 (2016).

[6] ALICE Collaboration, S. Acharya *et al.*, Production of $\mathrm{K}^*(892)^0$ and $\phi(1020)$ in pp and Pb–Pb collisions at $\sqrt{s_{\rm NN}} = 5.02$ TeV, Phys. Rev. C **106**, 034907 (2022).

[7] ALICE Collaboration, S. Acharya *et al.*, Multiplicity dependence of light-flavor hadron production in pp collisions at $\sqrt{s} = 7$ TeV, Phys. Rev. C **99**, 024906 (2019).

[8] ALICE Collaboration, S. Acharya *et al.*, Multiplicity dependence of (multi-)strange hadron production in proton-proton collisions at $\sqrt{s} = 13$ TeV, Eur. Phys. J. C **80**, 167 (2020).

[9] STAR Collaboration, K. H. Ackermann *et al.*, Elliptic flow in Au+Au collisions at $\sqrt{s_{\rm NN}} = 130$ GeV, Phys. Rev. Lett. **86**, 402 (2001).

[10] STAR Collaboration, J. Adams *et al.*, Experimental and theoretical challenges in the search for the quark gluon plasma: The STAR Collaboration's critical assessment of the evidence from RHIC collisions, Nucl. Phys. A **757**, 102 (2005).

[11] STAR Collaboration, J. Adams *et al.*, Evidence from d+Au measurements for final state suppression of high $p_{\rm T}$ hadrons in Au+Au collisions at RHIC, Phys. Rev. Lett. **91**, 072304 (2003).

[12] STAR Collaboration, C. Adler *et al.*, Disappearance of back-to-back high p_T hadron correlations in central Au+Au collisions at $\sqrt{s_{NN}} = 200$ GeV, Phys. Rev. Lett. **90**, 082302 (2003).

[13] STAR Collaboration, J. Adams *et al.*, Particle type dependence of azimuthal anisotropy and nuclear modification of particle production in Au+Au collisions at $\sqrt{s_{NN}} = 200$ GeV, Phys. Rev. Lett. **92**, 052302 (2004).

[14] PHENIX Collaboration, K. Adcox *et al.*, Suppression of hadrons with large transverse momentum in central Au+Au collisions at $\sqrt{s_{NN}} = 130$ GeV, Phys. Rev. Lett. **88**, 022301 (2001).

[15] PHENIX Collaboration, K. Adcox *et al.*, Formation of dense partonic matter in relativistic nucleus-nucleus collisions at RHIC: Experimental evaluation by the PHENIX collaboration, Nucl. Phys. A **757**, 184 (2005).

[16] BRAHMS Collaboration, I. Arsene *et al.*, Quark gluon plasma and color glass condensate at RHIC? The Perspective from the BRAHMS experiment, Nucl. Phys. A **757**, 1 (2005).

[17] PHOBOS Collaboration, B. B. Back *et al.*, The PHOBOS perspective on discoveries at RHIC, Nucl. Phys. A **757**, 28 (2005).

[18] ALICE Collaboration, The ALICE experiment – A journey through QCD, arXiv:2211.04384 [nucl-ex].
[19] ALICE Collaboration, K. Aamodt *et al.*, Elliptic flow of charged particles in Pb–Pb collisions at 2.76 TeV, Phys. Rev. Lett. **105**, 252302 (2010).
[20] ALICE Collaboration, K. Aamodt *et al.*, Suppression of charged particle production at large transverse momentum in central Pb–Pb collisions at $\sqrt{s_{NN}} = 2.76$ TeV, Phys. Lett. B **696**, 30 (2011).
[21] ALICE Collaboration, K. Aamodt *et al.*, Higher harmonic anisotropic flow measurements of charged particles in Pb–Pb collisions at $\sqrt{s_{NN}} = 2.76$ TeV, Phys. Rev. Lett. **107**, 032301 (2011).
[22] U. W. Heinz, The strongly coupled quark-gluon plasma created at RHIC, J. Phys. A **42**, 214003 (2009).
[23] T. Niida and Y. Miake, Signatures of QGP at RHIC and the LHC, AAPPS Bull. **31**, 12 (2021).
[24] J. P. Blaizot and J.-Y. Ollitrault, Equation of state and hydrodynamics of quark gluon plasmas, Phys. Lett. B **191**, 21 (1987).
[25] D. A. Teaney, Viscous Hydrodynamics and the Quark Gluon Plasma, in *Quark-Gluon Plasma 4* (World Scientific, Singapore, 2010), pp. 207–266.
[26] V. Greco, C. M. Ko, and P. Levai, Parton coalescence and antiproton/pion anomaly at RHIC, Phys. Rev. Lett. **90**, 202302 (2003).
[27] V. Greco, C. M. Ko, and P. Levai, Parton coalescence at RHIC, Phys. Rev. C **68**, 034904 (2003).
[28] R. J. Fries, B. Muller, C. Nonaka, and S. A. Bass, Hadronization in heavy ion collisions: Recombination and fragmentation of partons, Phys. Rev. Lett. **90**, 202303 (2003).
[29] R. J. Fries, B. Muller, C. Nonaka, and S. A. Bass, Hadron production in heavy ion collisions: Fragmentation and recombination from a dense parton phase, Phys. Rev. C **68**, 044902 (2003).
[30] A. Andronic, P. Braun-Munzinger, K. Redlich, and J. Stachel, Decoding the phase structure of QCD via particle production at high energy, Nature (London) **561**, 321 (2018).
[31] HotQCD Collaboration, A. Bazavov *et al.*, Chiral crossover in QCD at zero and non-zero chemical potentials, Phys. Lett. B **795**, 15 (2019).
[32] D. Teaney, Chemical freezeout in heavy ion collisions, arXiv:nucl-th/0204023.
[33] J. Manninen and F. Becattini, Chemical freeze-out in ultra-relativistic heavy ion collisions at $\sqrt{s_{NN}} = 130$ and 200 GeV, Phys. Rev. C **78**, 054901 (2008).
[34] U. W. Heinz and G. Kestin, Jozso's legacy: Chemical and kinetic freeze-out in heavy-ion collisions, Eur. Phys. J. Spec. Top. **155**, 75 (2008).
[35] J. M. Karthein, P. Alba, V. Mantovani-Sarti, J. Noronha-Hostler, P. Parotto, I. Portillo-Vazquez, V. Vovchenko, V. Koch, and C. Ratti, Thermal-model-based characterization of heavy-ion-collision systems at chemical freeze-out, EPJ Web Conf. **259**, 11010 (2022).
[36] A. Keranen and F. Becattini, The canonical effect in statistical models for relativistic heavy ion collisions, J. Phys. G **28**, 2041 (2002).
[37] V. Vovchenko, B. Dönigus, and H. Stoecker, Canonical statistical model analysis of pp, p–Pb, and Pb–Pb collisions at energies available at the CERN Large Hadron Collider, Phys. Rev. C **100**, 054906 (2019).
[38] J. Cleymans, The thermal-statistical model for particle production, EPJ Web Conf. **7**, 01001 (2010).
[39] S. Das Gupta and A. Z. Mekjian, The thermodynamic model for relativistic heavy ion collisions, Phys. Rep. **72**, 131 (1981).
[40] E. Schnedermann, J. Sollfrank, and U. W. Heinz, Thermal phenomenology of hadrons from 200 A/GeV S+S collisions, Phys. Rev. C **48**, 2462 (1993).
[41] ALICE Collaboration, S. Acharya *et al.*, Production of charged pions, kaons, and (anti-)protons in Pb–Pb and inelastic pp collisions at $\sqrt{s_{NN}} = 5.02$ TeV, Phys. Rev. C **101**, 044907 (2020).
[42] J. Steinheimer, J. Aichelin, M. Bleicher, and H. Stöcker, Influence of the hadronic phase on observables in ultrarelativistic heavy ion collisions, Phys. Rev. C **95**, 064902 (2017).
[43] S. Vogel and M. Bleicher, Resonance absorption and regeneration in relativistic heavy ion collisions, arXiv:nucl-th/0505027.
[44] STAR Collaboration, B. I. Abelev *et al.*, Strange baryon resonance production in $\sqrt{s_{NN}} = 200$ GeV p+p and Au+Au collisions, Phys. Rev. Lett. **97**, 132301 (2006).
[45] ALICE Collaboration, S. Acharya *et al.*, Evidence of rescattering effect in Pb–Pb collisions at the LHC through production of $K^*(892)^0$ and $\phi(1020)$ mesons, Phys. Lett. B **802**, 135225 (2020).
[46] STAR Collaboration, J. Adams *et al.*, $K(892)^*$ resonance production in Au+Au and p+p collisions at $\sqrt{s_{NN}} = 200$ GeV at STAR, Phys. Rev. C **71**, 064902 (2005).
[47] B. Z. Kopeliovich, I. K. Potashnikova,I. Schmidt, H. J. Pirner, and K. Reygers, Pion-pion cross section from proton-proton collisions at the LHC, Phys. Rev. D **91**, 054030 (2015).
[48] D. Aston *et al.*, A study of $K^-\pi^+$ scattering in the reaction $K^-p \to K^-\pi^-$ n at 11 GeV/c, Nucl. Phys. B **296**, 493 (1988).
[49] S. D. Protopopescu, M. Alston-Garnjost, A. Barbaro-Galtieri, S. M. Flatte, J. H. Friedman, T. A. Lasinski, G. R. Lynch, M. S. Rabin, and F. T. Solmitz, $\pi\pi$ partial wave analysis from reactions $\pi^+p \to \pi^+\pi^-\Delta^{++}$ and $\pi^+p \to K^+ K^-\Delta^{++}$ at 7.1 GeV/c, Phys. Rev. D **7**, 1279 (1973).
[50] G. Torrieri and J. Rafelski, Strange hadron resonances as a signature of freezeout dynamics, Phys. Lett. B **509**, 239 (2001).
[51] C. Markert, What do we learn from resonance production in heavy ion collisions? J. Phys. G **31**, S169 (2005).
[52] ALICE Collaboration, B. Abelev *et al.*, $K^*(892)^0$ and $\phi(1020)$ production in Pb–Pb collisions at $\sqrt{s_{NN}} = 2.76$ TeV, Phys. Rev. C **91**, 024609 (2015).
[53] ALICE Collaboration, S. Acharya *et al.*, Multiplicity dependence of $K^*(892)^0$ and $\phi(1020)$ production in pp collisions at $\sqrt{s} = 13$ TeV, Phys. Lett. B **807**, 135501 (2020).
[54] ALICE Collaboration, S. Acharya *et al.*, $K^*(892)^0$ and $\phi(1020)$ production in p–Pb collisions at $\sqrt{s_{NN}} = 8.16$ TeV, Phys. Rev. C **107**, 055201 (2023).
[55] ALICE Collaboration, S. Acharya *et al.*, Multiplicity and rapidity dependence of $K^*(892)^0$ and $\phi(1020)$ production in p–Pb collisions at $\sqrt{s_{NN}} = 5.02$ TeV, Eur. Phys. J. C **83**, 540 (2023).
[56] NA49 Collaboration, C. Alt *et al.*, Energy dependence of ϕ meson production in central Pb+Pb collisions at $\sqrt{s_{NN}} = 6$ to 17 GeV, Phys. Rev. C **78**, 044907 (2008).
[57] NA49 Collaboration, S. V. Afanasiev *et al.*, Production of ϕ mesons in p+p, p+Pb and central Pb+Pb collisions at E(beam) = 158 A GeV, Phys. Lett. B **491**, 59 (2000).

[58] NA49 Collaboration, T. Anticic *et al.*, $K^*(892)^0$ and $\bar{K}^*(892)^0$ production in central Pb+Pb, Si+Si, C+C and inelastic p+p collisions at 158 A GeV, Phys. Rev. C **84**, 064909 (2011).

[59] PHENIX Collaboration, A. Adare *et al.*, Measurement of K_S^0 and K^{*0} in p+p, d+Au, and Cu+Cu collisions at $\sqrt{s_{NN}} = 200$ GeV, Phys. Rev. C **90**, 054905 (2014).

[60] PHENIX Collaboration, N. J. Abdulameer *et al.*, Measurement of ϕ-meson production in Cu+Au collisions at $\sqrt{s_{NN}} = 200$ GeV and U+U collisions at $\sqrt{s_{NN}} = 193$ GeV, Phys. Rev. C **107**, 014907 (2023).

[61] PHENIX Collaboration, U. Acharya *et al.*, Study of ϕ-meson production in p+Al, p+Au, d+Au, and ^{3}He+Au collisions at $\sqrt{s_{NN}} = 200$ GeV, Phys. Rev. C **106**, 014908 (2022).

[62] PHENIX Collaboration, A. Adare *et al.*, Nuclear modification factors of ϕ mesons in d+Au, Cu+Cu and Au+Au collisions at $\sqrt{s_{NN}} = 200$ GeV, Phys. Rev. C **83**, 024909 (2011).

[63] PHENIX Collaboration, S. S. Adler *et al.*, Production of ϕ mesons at mid-rapidity in $\sqrt{s_{NN}} = 200$ GeV Au+Au collisions at RHIC, Phys. Rev. C **72**, 014903 (2005).

[64] STAR Collaboration, B. I. Abelev *et al.*, Energy and system size dependence of ϕ meson production in Cu+Cu and Au+Au collisions, Phys. Lett. B **673**, 183 (2009).

[65] STAR Collaboration, B. I. Abelev *et al.*, Measurements of ϕ meson production in relativistic heavy-ion collisions at RHIC, Phys. Rev. C **79**, 064903 (2009).

[66] STAR Collaboration, C. Adler *et al.*, $K^*(892)^0$ production in relativistic heavy ion collisions at $\sqrt{s_{NN}} = 130$ GeV, Phys. Rev. C **66**, 061901(R) (2002).

[67] STAR Collaboration, M. M. Aggarwal *et al.*, K^{*0} production in Cu+Cu and Au+Au collisions at $\sqrt{s_{NN}} = 62.4$ GeV and 200 GeV, Phys. Rev. C **84**, 034909 (2011).

[68] ALICE Collaboration, J. Adam *et al.*, $K^*(892)^0$ and $\phi(1020)$ meson production at high transverse momentum in pp and Pb–Pb collisions at $\sqrt{s_{NN}} = 2.76$ TeV, Phys. Rev. C **95**, 064606 (2017).

[69] C. Loizides, J. Nagle, and P. Steinberg, Improved version of the PHOBOS Glauber Monte Carlo, SoftwareX **1–2**, 13 (2015).

[70] C. Loizides, J. Kamin, and D. d'Enterria, Improved Monte Carlo Glauber predictions at present and future nuclear colliders, Phys. Rev. C **97**, 054910 (2018); **99**, 019901(E) (2019).

[71] ALICE Collaboration, J. Adam *et al.*, Enhanced production of multi-strange hadrons in high-multiplicity proton-proton collisions, Nat. Phys. **13**, 535 (2017).

[72] ALICE Collaboration, S. Acharya *et al.*, Long- and short-range correlations and their event-scale dependence in high-multiplicity pp collisions at $\sqrt{s} = 13$ TeV, J. High Energy Phys. 05 (2021) 290.

[73] ALICE Collaboration, S. Acharya *et al.*, Investigations of anisotropic flow using multiparticle azimuthal correlations in pp, p–Pb, Xe–Xe, and Pb–Pb collisions at the LHC, Phys. Rev. Lett. **123**, 142301 (2019).

[74] PHENIX Collaboration, C. Aidala *et al.*, Creation of quark–gluon plasma droplets with three distinct geometries, Nat. Phys. **15**, 214 (2019).

[75] CMS Collaboration, V. Khachatryan *et al.*, Evidence for collectivity in pp collisions at the LHC, Phys. Lett. B **765**, 193 (2017).

[76] A. Motornenko, V. Vovchenko, C. Greiner, and H. Stoecker, Kinetic freeze-out temperature from yields of short-lived resonances, Phys. Rev. C **102**, 024909 (2020).

[77] ALICE Collaboration, B. B. Abelev *et al.*, Performance of the ALICE experiment at the CERN LHC, Int. J. Mod. Phys. A **29**, 1430044 (2014).

[78] ALICE Collaboration, K. Aamodt *et al.*, The ALICE experiment at the CERN LHC, JINST **3**, S08002 (2008).

[79] ALICE Collaboration, E. Abbas *et al.*, Performance of the ALICE VZERO system, J. Inst. **8**, P10016 (2013).

[80] ALICE Collaboration, S. Acharya *et al.*, Transverse momentum spectra and nuclear modification factors of charged particles in Xe–Xe collisions at $\sqrt{s_{NN}} = 5.44$ TeV, Phys. Lett. B **788**, 166 (2019).

[81] ALICE Collaboration, J. Adam *et al.*, Pseudorapidity and transverse-momentum distributions of charged particles in proton–proton collisions at $\sqrt{s} = 13$ TeV, Phys. Lett. B **753**, 319 (2016).

[82] ALICE Collaboration, B. Abelev *et al.*, Technical design report for the upgrade of the ALICE inner tracking system, J. Phys. G **41**, 087002 (2014).

[83] ALICE Collaboration, S. Acharya *et al.*, Centrality and pseudorapidity dependence of the charged-particle multiplicity density in Xe–Xe collisions at $\sqrt{s_{NN}} = 5.44$ TeV, Phys. Lett. B **790**, 35 (2019).

[84] ALICE Collaboration, S. Acharya *et al.*, Charged-particle production as a function of multiplicity and transverse spherocity in pp collisions at $\sqrt{s} = 5.02$ and 13 TeV, Eur. Phys. J. C **79**, 857 (2019).

[85] J. Alme *et al.*, The ALICE TPC, a large 3-dimensional tracking device with fast readout for ultra-high multiplicity events, Nucl. Instrum. Methods Phys. Res. A **622**, 316 (2010).

[86] ALICE Collaboration, S. Acharya *et al.*, Production of pions, kaons, (anti-)protons and ϕ mesons in Xe–Xe collisions at $\sqrt{s_{NN}} = 5.44$ TeV, Eur. Phys. J. C **81**, 584 (2021).

[87] ALICE Collaboration, G. Dellacasa *et al.*, ALICE technical design report of the time-of-flight system (TOF), No. CERN-LHCC-2000-012.

[88] ALICE Collaboration, F. Carnesecchi, Performance of the ALICE time-of-flight detector at the LHC, J. Inst. **14**, C06023 (2019).

[89] Particle Data Group, R. L. Workman *et al.*, Review of particle physics, PTEP **2022**, 083C01 (2022).

[90] P. Skands, S. Carrazza, and J. Rojo, Tuning PYTHIA 8.1: The Monash 2013 Tune, Eur. Phys. J. C **74**, 3024 (2014).

[91] X.-N. Wang and M. Gyulassy, HIJING: A Monte Carlo model for multiple jet production in pp, pA and AA collisions, Phys. Rev. D **44**, 3501 (1991).

[92] R. Brun, F. Bruyant, F. Carminati, S. Giani, M. Maire, A. McPherson, G. Patrick, and L. Urban, GEANT Detector Description and Simulation Tool, CERN Program Library, CERN, Geneva (1993).

[93] C. Tsallis, Possible generalization of Boltzmann-Gibbs statistics, J. Stat. Phys. **52**, 479 (1988).

[94] ALICE Collaboration, S. Acharya *et al.*, Production of light-flavor hadrons in pp collisions at $\sqrt{s} = 7$ and $\sqrt{s} = 13$ TeV, Eur. Phys. J. C **81**, 256 (2021).

[95] ALICE Collaboration, K. Aamodt *et al.*, Two-pion Bose-Einstein correlations in central Pb–Pb collisions at $\sqrt{s_{NN}} = 2.76$ TeV, Phys. Lett. B **696**, 328 (2011).

[96] ALICE Collaboration, S. Acharya *et al.*, Multiplicity dependence of π, K, and p production in pp collisions at $\sqrt{s} = 13$ TeV, Eur. Phys. J. C **80**, 693 (2020).

[97] U. W. Heinz and J. S. Moreland, Hydrodynamic flow in small systems or: "How the heck is it possible that a system emitting only a dozen particles can be described by fluid dynamics?", J. Phys.: Conf. Ser. **1271**, 012018 (2019).

[98] A. G. Knospe, C. Markert, K. Werner, J. Steinheimer, and M. Bleicher, Hadronic resonance production and interaction in partonic and hadronic matter in the EPOS3 model with and without the hadronic afterburner UrQMD, Phys. Rev. C **93**, 014911 (2016).

[99] M. Bleicher *et al.*, Relativistic hadron hadron collisions in the ultrarelativistic quantum molecular dynamics model, J. Phys. G **25**, 1859 (1999).

[100] ALICE Collaboration, S. Acharya *et al.*, $K^*(892)^{\pm}$ resonance production in Pb−Pb collisions at $\sqrt{s_{NN}} = 5.02$ TeV, arXiv:2308.16119.

[101] F. A. Flor, G. Olinger, and R. Bellwied, System size and flavour dependence of chemical freeze-out temperatures in ALICE data from pp, pPb and PbPb collisions at LHC energies, Phys. Lett. B **834**, 137473 (2022).

[102] V. Vovchenko, B. Dönigus, and H. Stoecker, Multiplicity dependence of light nuclei production at LHC energies in the canonical statistical model, Phys. Lett. B **785**, 171 (2018).

[103] A. Tawfik, Matter-antimatter asymmetry in heavy-ion collisions, Int. J. Theor. Phys. **51**, 1396 (2012).

S. Acharya,[128] D. Adamová,[87] G. Aglieri Rinella,[33] M. Agnello,[30] N. Agrawal,[52] Z. Ahammed,[136] S. Ahmad,[16] S. U. Ahn,[72] I. Ahuja,[38] A. Akindinov,[142] M. Al-Turany,[98] D. Aleksandrov,[142] B. Alessandro,[57] H. M. Alfanda,[6] R. Alfaro Molina,[68] B. Ali,[16] A. Alici,[26] N. Alizadehvandchali,[117] A. Alkin,[33] J. Alme,[21] G. Alocco,[53] T. Alt,[65] A. R. Altamura,[51] I. Altsybeev,[96] J. R. Alvarado,[45] M. N. Anaam,[6] C. Andrei,[46] N. Andreou,[116] A. Andronic,[127] V. Anguelov,[95] F. Antinori,[55] P. Antonioli,[52] N. Apadula,[75] L. Aphecetche,[104] H. Appelshäuser,[65] C. Arata,[74] S. Arcelli,[26] M. Aresti,[23] R. Arnaldi,[57] J. G. M. C. A. Arneiro,[111] I. C. Arsene,[20] M. Arslandok,[139] A. Augustinus,[33] R. Averbeck,[98] M. D. Azmi,[16] H. Baba,[125] A. Badalà,[54] J. Bae,[105] Y. W. Baek,[41] X. Bai,[121] R. Bailhache,[65] Y. Bailung,[49] A. Balbino,[30] A. Baldisseri,[131] B. Balis,[2] D. Banerjee,[4] Z. Banoo,[92] R. Barbera,[27] F. Barile,[32] L. Barioglio,[96] M. Barlou,[79] B. Barman,[42] G. G. Barnaföldi,[47] L. S. Barnby,[86] V. Barret,[128] L. Barreto,[111] C. Bartels,[120] K. Barth,[33] E. Bartsch,[65] N. Bastid,[128] S. Basu,[76] G. Batigne,[104] D. Battistini,[96] B. Batyunya,[143] D. Bauri,[48] J. L. Bazo Alba,[102] I. G. Bearden,[84] C. Beattie,[139] P. Becht,[98] D. Behera,[49] I. Belikov,[130] A. D. C. Bell Hechavarria,[127] F. Bellini,[26] R. Bellwied,[117] S. Belokurova,[142] Y. A. V. Beltran,[45] G. Bencedi,[47] S. Beole,[25] Y. Berdnikov,[142] A. Berdnikova,[95] L. Bergmann,[95] M. G. Besoiu,[64] L. Betev,[33] P. P. Bhaduri,[136] A. Bhasin,[92] M. A. Bhat,[4] B. Bhattacharjee,[42] L. Bianchi,[25] N. Bianchi,[50] J. Bielčík,[36] J. Bielčíková,[87] J. Biernat,[108] A. P. Bigot,[130] A. Bilandzic,[96] G. Biro,[47] S. Biswas,[4] N. Bize,[104] J. T. Blair,[109] D. Blau,[142] M. B. Blidaru,[98] N. Bluhme,[39] C. Blume,[65] G. Boca,[22,56] F. Bock,[88] T. Bodova,[21] A. Bogdanov,[142] S. Boi,[23] J. Bok,[59] L. Boldizsár,[47] M. Bombara,[38] P. M. Bond,[33] G. Bonomi,[135,56] H. Borel,[131] A. Borissov,[142] A. G. Borquez Carcamo,[95] H. Bossi,[139] E. Botta,[25] Y. E. M. Bouziani,[65] L. Bratrud,[65] P. Braun-Munzinger,[98] M. Bregant,[111] M. Broz,[36] G. E. Bruno,[97,32] M. D. Buckland,[24] D. Budnikov,[142] H. Buesching,[65] S. Bufalino,[30] P. Buhler,[103] N. Burmasov,[142] Z. Buthelezi,[69,124] A. Bylinkin,[21] S. A. Bysiak,[108] M. Cai,[6] H. Caines,[139] A. Caliva,[29] E. Calvo Villar,[102] J. M. M. Camacho,[110] P. Camerini,[24] F. D. M. Canedo,[111] S. L. Cantway,[139] M. Carabas,[114] A. A. Carballo,[33] F. Carnesecchi,[33] R. Caron,[129] L. A. D. Carvalho,[111] J. Castillo Castellanos,[131] F. Catalano,[33,25] C. Ceballos Sanchez,[143] I. Chakaberia,[75] P. Chakraborty,[48] S. Chandra,[136] S. Chapeland,[33] M. Chartier,[120] S. Chattopadhyay,[136] S. Chattopadhyay,[100] T. Cheng,[98,6] C. Cheshkov,[129] B. Cheynis,[129] V. Chibante Barroso,[33] D. D. Chinellato,[112] E. S. Chizzali,[96,*] J. Cho,[59] S. Cho,[59] P. Chochula,[33] D. Choudhury,[42] P. Christakoglou,[85] C. H. Christensen,[84] P. Christiansen,[76] T. Chujo,[126] M. Ciacco,[30] C. Cicalo,[53] F. Cindolo,[52] M. R. Ciupek,[98] G. Clai,[52,†] F. Colamaria,[51] J. S. Colburn,[101] D. Colella,[97,32] M. Colocci,[26] M. Concas,[33,‡] G. Conesa Balbastre,[74] Z. Conesa del Valle,[132] G. Contin,[24] J. G. Contreras,[36] M. L. Coquet,[131] P. Cortese,[134,57] M. R. Cosentino,[113] F. Costa,[33] S. Costanza,[22,56] C. Cot,[132] J. Crkovská,[95] P. Crochet,[128] R. Cruz-Torres,[75] P. Cui,[6] A. Dainese,[55] M. C. Danisch,[95] A. Danu,[64] P. Das,[81] P. Das,[4] S. Das,[4] A. R. Dash,[127] S. Dash,[48] A. De Caro,[29] G. de Cataldo,[51] J. de Cuveland,[39] A. De Falco,[23] D. De Gruttola,[29] N. De Marco,[57] C. De Martin,[24] S. De Pasquale,[29] R. Deb,[135] R. Del Grande,[96] L. Dello Stritto,[29] W. Deng,[6] P. Dhankher,[19] D. Di Bari,[32] A. Di Mauro,[33] B. Diab,[131] R. A. Diaz,[143,7] T. Dietel,[115] Y. Ding,[6] J. Ditzel,[65] R. Divià,[33] D. U. Dixit,[19] Ø. Djuvsland,[21] U. Dmitrieva,[142] A. Dobrin,[64] B. Dönigus,[65] J. M. Dubinski,[137] A. Dubla,[98] S. Dudi,[91] P. Dupieux,[128] M. Durkac,[107] N. Dzalaiova,[13] T. M. Eder,[127] R. J. Ehlers,[75] F. Eisenhut,[65] R. Ejima,[93] D. Elia,[51] B. Erazmus,[104] F. Ercolessi,[26] B. Espagnon,[132] G. Eulisse,[33] D. Evans,[101] S. Evdokimov,[142] L. Fabbietti,[96] M. Faggin,[28] J. Faivre,[74] F. Fan,[6] W. Fan,[75] A. Fantoni,[50] M. Fasel,[88] P. Fecchio,[30] A. Feliciello,[57] G. Feofilov,[142] A. Fernández Téllez,[45] L. Ferrandi,[111] M. B. Ferrer,[33] A. Ferrero,[131] C. Ferrero,[57] A. Ferretti,[25] V. J. G. Feuillard,[95] V. Filova,[36] D. Finogeev,[142] F. M. Fionda,[53] E. Flatland,[33] F. Flor,[117] A. N. Flores,[109] S. Foertsch,[69] I. Fokin,[95] S. Fokin,[142] E. Fragiacomo,[58] E. Frajna,[47] U. Fuchs,[33] N. Funicello,[29] C. Furget,[74] A. Furs,[142] T. Fusayasu,[99] J. J. Gaardhøje,[84] M. Gagliardi,[25] A. M. Gago,[102] T. Gahlaut,[48] C. D. Galvan,[110] D. R. Gangadharan,[117] P. Ganoti,[79] C. Garabatos,[98] T. García Chávez,[45] E. Garcia-Solis,[9] C. Gargiulo,[33] P. Gasik,[98] A. Gautam,[119] M. B. Gay Ducati,[67] M. Germain,[104] A. Ghimouz,[126] C. Ghosh,[136] M. Giacalone,[52]

G. Gioachin,[30] P. Giubellino,[98,57] P. Giubilato,[28] A. M. C. Glaenzer,[131] P. Glässel,[95] E. Glimos,[123] D. J. Q. Goh,[77] V. Gonzalez,[138] M. Gorgon,[2] K. Goswami,[49] S. Gotovac,[34] V. Grabski,[68] L. K. Graczykowski,[137] E. Grecka,[87] A. Grelli,[60] C. Grigoras,[33] V. Grigoriev,[142] S. Grigoryan,[143,1] F. Grosa,[33] J. F. Grosse-Oetringhaus,[33] R. Grosso,[98] D. Grund,[36] N. A. Grunwald,[95] G. G. Guardiano,[112] R. Guernane,[74] M. Guilbaud,[104] K. Gulbrandsen,[84] T. Gündem,[65] T. Gunji,[125] W. Guo,[6] A. Gupta,[92] R. Gupta,[92] R. Gupta,[49] K. Gwizdziel,[137] L. Gyulai,[47] C. Hadjidakis,[132] F. U. Haider,[92] S. Haidlova,[36] H. Hamagaki,[77] A. Hamdi,[75] Y. Han,[140] B. G. Hanley,[138] R. Hannigan,[109] J. Hansen,[76] M. R. Haque,[137] J. W. Harris,[139] A. Harton,[9] H. Hassan,[118] D. Hatzifotiadou,[52] P. Hauer,[43] L. B. Havener,[139] S. T. Heckel,[96] E. Hellbär,[98] H. Helstrup,[35] M. Hemmer,[65] T. Herman,[36] G. Herrera Corral,[8] F. Herrmann,[127] S. Herrmann,[129] K. F. Hetland,[35] B. Heybeck,[65] H. Hillemanns,[33] B. Hippolyte,[130] F. W. Hoffmann,[71] B. Hofman,[60] G. H. Hong,[140] M. Horst,[96] A. Horzyk,[2] Y. Hou,[6] P. Hristov,[33] C. Hughes,[123] P. Huhn,[65] L. M. Huhta,[118] T. J. Humanic,[89] A. Hutson,[117] D. Hutter,[39] R. Ilkaev,[142] H. Ilyas,[14] M. Inaba,[126] G. M. Innocenti,[33] M. Ippolitov,[142] A. Isakov,[85,87] T. Isidori,[119] M. S. Islam,[100] M. Ivanov,[13] M. Ivanov,[98] V. Ivanov,[142] K. E. Iversen,[76] M. Jablonski,[2] B. Jacak,[75] N. Jacazio,[26] P. M. Jacobs,[75] S. Jadlovska,[107] J. Jadlovsky,[107] S. Jaelani,[83] C. Jahnke,[111] M. J. Jakubowska,[137] M. A. Janik,[137] T. Janson,[71] S. Ji,[17] S. Jia,[10] A. A. P. Jimenez,[66] F. Jonas,[88,127] D. M. Jones,[120] J. M. Jowett,[33,98] J. Jung,[65] M. Jung,[65] A. Junique,[33] A. Jusko,[101] M. J. Kabus,[33,137] J. Kaewjai,[106] P. Kalinak,[61] A. S. Kalteyer,[98] A. Kalweit,[33] V. Kaplin,[142] A. Karasu Uysal,[73] D. Karatovic,[90] O. Karavichev,[142] T. Karavicheva,[142] P. Karczmarczyk,[137] E. Karpechev,[142] U. Kebschull,[71] R. Keidel,[141] D. L. D. Keijdener,[60] M. Keil,[33] B. Ketzer,[43] S. S. Khade,[49] A. M. Khan,[121] S. Khan,[16] A. Khanzadeev,[142] Y. Kharlov,[142] A. Khatun,[119] A. Khuntia,[36] B. Kileng,[35] B. Kim,[105] C. Kim,[17] D. J. Kim,[118] E. J. Kim,[70] J. Kim,[140] J. S. Kim,[41] J. Kim,[59] J. Kim,[70] M. Kim,[19] S. Kim,[18] T. Kim,[140] K. Kimura,[93] S. Kirsch,[65] I. Kisel,[39] S. Kiselev,[142] A. Kisiel,[137] J. P. Kitowski,[2] J. L. Klay,[5] J. Klein,[33] S. Klein,[75] C. Klein-Bösing,[127] M. Kleiner,[65] T. Klemenz,[96] A. Kluge,[33] A. G. Knospe,[117] C. Kobdaj,[106] T. Kollegger,[98] A. Kondratyev,[143] N. Kondratyeva,[142] E. Kondratyuk,[142] J. Konig,[65] S. A. Konigstorfer,[96] P. J. Konopka,[33] G. Kornakov,[137] M. Korwieser,[96] S. D. Koryciak,[2] A. Kotliarov,[87] V. Kovalenko,[142] M. Kowalski,[108] V. Kozhuharov,[37] I. Králik,[61] A. Kravčáková,[38] L. Krcal,[33,39] M. Krivda,[101,61] F. Krizek,[87] K. Krizkova Gajdosova,[33] M. Kroesen,[95] M. Krüger,[65] D. M. Krupova,[36] E. Kryshen,[142] V. Kučera,[59] C. Kuhn,[130] P. G. Kuijer,[85] T. Kumaoka,[126] D. Kumar,[136] L. Kumar,[91] N. Kumar,[91] S. Kumar,[32] S. Kundu,[33] P. Kurashvili,[80] A. Kurepin,[142] A. B. Kurepin,[142] A. Kuryakin,[142] S. Kushpil,[87] M. J. Kweon,[59] Y. Kwon,[140] S. L. La Pointe,[39] P. La Rocca,[27] A. Lakrathok,[106] M. Lamanna,[33] A. R. Landou,[74,116] R. Langoy,[122] P. Larionov,[33] E. Laudi,[33] L. Lautner,[33,96] R. Lavicka,[103] R. Lea,[135,56] H. Lee,[105] I. Legrand,[46] G. Legras,[127] J. Lehrbach,[39] T. M. Lelek,[2] R. C. Lemmon,[86] I. León Monzón,[110] M. M. Lesch,[96] E. D. Lesser,[19] P. Lévai,[47] X. Li,[10] J. Lien,[122] R. Lietava,[101] I. Likmeta,[117] B. Lim,[25] S. H. Lim,[17] V. Lindenstruth,[39] A. Lindner,[46] C. Lippmann,[98] D. H. Liu,[6] J. Liu,[120] G. S. S. Liveraro,[112] I. M. Lofnes,[21] C. Loizides,[88] S. Lokos,[108] J. Lömker,[60] P. Loncar,[34] X. Lopez,[128] E. López Torres,[7] P. Lu,[98,121] F. V. Lugo,[68] J. R. Luhder,[127] M. Lunardon,[28] G. Luparello,[58] Y. G. Ma,[40] M. Mager,[33] A. Maire,[130] E. M. Majerz,[2] M. V. Makariev,[37] M. Malaev,[142] G. Malfattore,[26] N. M. Malik,[92] Q. W. Malik,[20] S. K. Malik,[92] L. Malinina,[143,§] D. Mallick,[132,81] N. Mallick,[49] G. Mandaglio,[31,54] S. K. Mandal,[80] V. Manko,[142] F. Manso,[128] V. Manzari,[51] Y. Mao,[6] R. W. Marcjan,[2] G. V. Margagliotti,[24] A. Margotti,[52] A. Marín,[98] C. Markert,[109] P. Martinengo,[33] M. I. Martínez,[45] G. Martínez García,[104] M. P. P. Martins,[111] S. Masciocchi,[98] M. Masera,[25] A. Masoni,[53] L. Massacrier,[132] O. Massen,[60] A. Mastroserio,[133,51] O. Matonoha,[76] S. Mattiazzo,[28] A. Matyja,[108] C. Mayer,[108] A. L. Mazuecos,[33] F. Mazzaschi,[25] M. Mazzilli,[33] J. E. Mdhluli,[124] Y. Melikyan,[44] A. Menchaca-Rocha,[68] J. E. M. Mendez,[66] E. Meninno,[103] A. S. Menon,[117] M. Meres,[13] S. Mhlanga,[115,69] Y. Miake,[126] L. Micheletti,[33] D. L. Mihaylov,[96] K. Mikhaylov,[143,142] A. N. Mishra,[47] D. Miśkowiec,[98] A. Modak,[4] B. Mohanty,[81] M. Mohisin Khan,[16,‖] M. A. Molander,[44] S. Monira,[137] C. Mordasini,[118] D. A. Moreira De Godoy,[127] I. Morozov,[142] A. Morsch,[33] T. Mrnjavac,[33] V. Muccifora,[50] S. Muhuri,[136] J. D. Mulligan,[75] A. Mulliri,[23] M. G. Munhoz,[111] R. H. Munzer,[65] H. Murakami,[125] S. Murray,[115] L. Musa,[33] J. Musinsky,[61] J. W. Myrcha,[137] B. Naik,[124] A. I. Nambrath,[19] B. K. Nandi,[48] R. Nania,[52] E. Nappi,[51] A. F. Nassirpour,[18] A. Nath,[95] C. Nattrass,[123] M. N. Naydenov,[37] A. Neagu,[20] A. Negru,[114] L. Nellen,[66] R. Nepeivoda,[76] S. Nese,[20] G. Neskovic,[39] N. Nicassio,[51] B. S. Nielsen,[84] E. G. Nielsen,[84] S. Nikolaev,[142] S. Nikulin,[142] V. Nikulin,[142] F. Noferini,[52] S. Noh,[12] P. Nomokonov,[143] J. Norman,[120] N. Novitzky,[88] P. Nowakowski,[137] A. Nyanin,[142] J. Nystrand,[21] M. Ogino,[77] S. Oh,[18] A. Ohlson,[76] V. A. Okorokov,[142] J. Oleniacz,[137] A. C. Oliveira Da Silva,[123] A. Onnerstad,[118] C. Oppedisano,[57] A. Ortiz Velasquez,[66] J. Otwinowski,[108] M. Oya,[93] K. Oyama,[77] Y. Pachmayer,[95] S. Padhan,[48] D. Pagano,[135,56] G. Paić,[66] S. Paisano-Guzmán,[45] A. Palasciano,[51] S. Panebianco,[131] H. Park,[126] H. Park,[105] J. Park,[59] J. E. Parkkila,[33] Y. Patley,[48] R. N. Patra,[92] B. Paul,[23] H. Pei,[6] T. Peitzmann,[60] X. Peng,[11] M. Pennisi,[25] S. Perciballi,[25] D. Peresunko,[142] G. M. Perez,[7] Y. Pestov,[142] V. Petrov,[142] M. Petrovici,[46] R. P. Pezzi,[104,67] S. Piano,[58] M. Pikna,[13] P. Pillot,[104] O. Pinazza,[52,33] L. Pinsky,[117] C. Pinto,[96] S. Pisano,[50] M. Płoskoń,[75] M. Planinic,[90] F. Pliquett,[65] M. G. Poghosyan,[88] B. Polichtchouk,[142] S. Politano,[30] N. Poljak,[90] A. Pop,[46] S. Porteboeuf-Houssais,[128] V. Pozdniakov,[143] I. Y. Pozos,[45] K. K. Pradhan,[49] S. K. Prasad,[4] S. Prasad,[49]

R. Preghenella,[52] F. Prino,[57] C. A. Pruneau,[138] I. Pshenichnov,[142] M. Puccio,[33] S. Pucillo,[25] Z. Pugelova,[107] S. Qiu,[85] L. Quaglia,[25] S. Ragoni,[15] A. Rai,[139] A. Rakotozafindrabe,[131] L. Ramello,[134,57] F. Rami,[130] T. A. Rancien,[74] M. Rasa,[27] S. S. Räsänen,[44] R. Rath,[52] M. P. Rauch,[21] I. Ravasenga,[85] K. F. Read,[88,123] C. Reckziegel,[113] A. R. Redelbach,[39] K. Redlich,[80,¶] C. A. Reetz,[98] H. D. Regules-Medel,[45] A. Rehman,[21] F. Reidt,[33] H. A. Reme-Ness,[35] Z. Rescakova,[38] K. Reygers,[95] A. Riabov,[142] V. Riabov,[142] R. Ricci,[29] M. Richter,[20] A. A. Riedel,[96] W. Riegler,[33] A. G. Riffero,[25] C. Ristea,[64] M. V. Rodriguez,[33] M. Rodríguez Cahuantzi,[45] S. A. Rodríguez Ramírez,[45] K. Røed,[20] R. Rogalev,[142] E. Rogochaya,[143] T. S. Rogoschinski,[65] D. Rohr,[33] D. Röhrich,[21] P. F. Rojas,[45] S. Rojas Torres,[36] P. S. Rokita,[137] G. Romanenko,[26] F. Ronchetti,[50] A. Rosano,[31,54] E. D. Rosas,[66] K. Roslon,[137] A. Rossi,[55] A. Roy,[49] S. Roy,[48] N. Rubini,[26] D. Ruggiano,[137] R. Rui,[24] P. G. Russek,[2] R. Russo,[85] A. Rustamov,[82] E. Ryabinkin,[142] Y. Ryabov,[142] A. Rybicki,[108] H. Rytkonen,[118] J. Ryu,[17] W. Rzesa,[137] O. A. M. Saarimaki,[44] S. Sadhu,[32] S. Sadovsky,[142] J. Saetre,[21] K. Šafařík,[36] P. Saha,[42] S. K. Saha,[4] S. Saha,[81] B. Sahoo,[48] B. Sahoo,[49] R. Sahoo,[49] S. Sahoo,[62] D. Sahu,[49] P. K. Sahu,[62] J. Saini,[136] K. Sajdakova,[38] S. Sakai,[126] M. P. Salvan,[98] S. Sambyal,[92] D. Samitz,[103] I. Sanna,[33,96] T. B. Saramela,[111] P. Sarma,[42] V. Sarritzu,[23] V. M. Sarti,[96] M. H. P. Sas,[33] S. Sawan,[81] J. Schambach,[88] H. S. Scheid,[65] C. Schiaua,[46] R. Schicker,[95] F. Schlepper,[95] A. Schmah,[98] C. Schmidt,[98] H. R. Schmidt,[94] M. O. Schmidt,[33] M. Schmidt,[94] N. V. Schmidt,[88] A. R. Schmier,[123] R. Schotter,[130] A. Schröter,[39] J. Schukraft,[33] K. Schweda,[98] G. Scioli,[26] E. Scomparin,[57] J. E. Seger,[15] Y. Sekiguchi,[125] D. Sekihata,[125] M. Selina,[85] I. Selyuzhenkov,[98] S. Senyukov,[130] J. J. Seo,[95,59] D. Serebryakov,[142] L. Šerkšnytė,[96] A. Sevcenco,[64] T. J. Shaba,[69] A. Shabetai,[104] R. Shahoyan,[33] A. Shangaraev,[142] A. Sharma,[91] B. Sharma,[92] D. Sharma,[48] H. Sharma,[55,108] M. Sharma,[92] S. Sharma,[77] S. Sharma,[92] U. Sharma,[92] A. Shatat,[132] O. Sheibani,[117] K. Shigaki,[93] M. Shimomura,[78] J. Shin,[12] S. Shirinkin,[142] Q. Shou,[40] Y. Sibiriak,[142] S. Siddhanta,[53] T. Siemiarczuk,[80] T. F. Silva,[111] D. Silvermyr,[76] T. Simantathammakul,[106] R. Simeonov,[37] B. Singh,[92] B. Singh,[96] K. Singh,[49] R. Singh,[81] R. Singh,[92] R. Singh,[49] S. Singh,[16] V. K. Singh,[136] V. Singhal,[136] T. Sinha,[100] B. Sitar,[13] M. Sitta,[134,57] T. B. Skaali,[20] G. Skorodumovs,[95] M. Slupecki,[44] N. Smirnov,[139] R. J. M. Snellings,[60] E. H. Solheim,[20] J. Song,[17] C. Sonnabend,[33,98] F. Soramel,[28] A. B. Soto-hernandez,[89] R. Spijkers,[85] I. Sputowska,[108] J. Staa,[76] J. Stachel,[95] I. Stan,[64] P. J. Steffanic,[123] S. F. Stiefelmaier,[95] D. Stocco,[104] I. Storehaug,[20] P. Stratmann,[127] S. Strazzi,[26] A. Sturniolo,[31,54] C. P. Stylianidis,[85] A. A. P. Suaide,[111] C. Suire,[132] M. Sukhanov,[142] M. Suljic,[33] R. Sultanov,[142] V. Sumberia,[92] S. Sumowidagdo,[83] S. Swain,[62] I. Szarka,[13] M. Szymkowski,[137] S. F. Taghavi,[96] G. Taillepied,[98] J. Takahashi,[112] G. J. Tambave,[81] S. Tang,[6] Z. Tang,[121] J. D. Tapia Takaki,[119] N. Tapus,[114] L. A. Tarasovicova,[127] M. G. Tarzila,[46] G. F. Tassielli,[32] A. Tauro,[33] A. Tavira García,[132] G. Tejeda Muñoz,[45] A. Telesca,[33] L. Terlizzi,[25] C. Terrevoli,[117] S. Thakur,[4] D. Thomas,[109] A. Tikhonov,[142] N. Tiltmann,[127] A. R. Timmins,[117] M. Tkacik,[107] T. Tkacik,[107] A. Toia,[65] R. Tokumoto,[93] K. Tomohiro,[93] N. Topilskaya,[142] M. Toppi,[50] T. Tork,[132] P. V. Torres,[66] V. V. Torres,[104] A. G. Torres Ramos,[32] A. Trifiró,[31,54] A. S. Triolo,[33,31,54] S. Tripathy,[52] T. Tripathy,[48] S. Trogolo,[33] V. Trubnikov,[3] W. H. Trzaska,[118] T. P. Trzcinski,[137] A. Tumkin,[142] R. Turrisi,[55] T. S. Tveter,[20] K. Ullaland,[21] B. Ulukutlu,[96] A. Uras,[129] G. L. Usai,[23] M. Vala,[38] N. Valle,[22] L. V. R. van Doremalen,[60] M. van Leeuwen,[85] C. A. van Veen,[95] R. J. G. van Weelden,[85] P. Vande Vyvre,[33] D. Varga,[47] Z. Varga,[47] M. Vasileiou,[79] A. Vasiliev,[142] O. Vázquez Doce,[50] O. Vazquez Rueda,[117] V. Vechernin,[142] E. Vercellin,[25] S. Vergara Limón,[45] R. Verma,[48] L. Vermunt,[98] R. Vértesi,[47] M. Verweij,[60] L. Vickovic,[34] Z. Vilakazi,[124] O. Villalobos Baillie,[101] A. Villani,[24] A. Vinogradov,[142] T. Virgili,[29] M. M. O. Virta,[118] V. Vislavicius,[76] A. Vodopyanov,[143] B. Volkel,[33] M. A. Völkl,[95] K. Voloshin,[142] S. A. Voloshin,[138] G. Volpe,[32] B. von Haller,[33] I. Vorobyev,[96] N. Vozniuk,[142] J. Vrláková,[38] J. Wan,[40] C. Wang,[40] D. Wang,[40] Y. Wang,[40] Y. Wang,[6] A. Wegrzynek,[33] F. T. Weiglhofer,[39] S. C. Wenzel,[33] J. P. Wessels,[127] J. Wiechula,[65] J. Wikne,[20] G. Wilk,[80] J. Wilkinson,[98] G. A. Willems,[127] B. Windelband,[95] M. Winn,[131] J. R. Wright,[109] W. Wu,[40] Y. Wu,[121] R. Xu,[6] A. Yadav,[43] A. K. Yadav,[136] S. Yalcin,[73] Y. Yamaguchi,[93] S. Yang,[21] S. Yano,[93] Z. Yin,[6] I.-K. Yoo,[17] J. H. Yoon,[59] H. Yu,[12] S. Yuan,[21] A. Yuncu,[95] V. Zaccolo,[24] C. Zampolli,[33] F. Zanone,[95] N. Zardoshti,[33] A. Zarochentsev,[142] P. Závada,[63] N. Zaviyalov,[142] M. Zhalov,[142] B. Zhang,[6] C. Zhang,[131] L. Zhang,[40] S. Zhang,[40] X. Zhang,[6] Y. Zhang,[121] Z. Zhang,[6] M. Zhao,[10] V. Zherebchevskii,[142] Y. Zhi,[10] D. Zhou,[6] Y. Zhou,[84] J. Zhu,[55,6] Y. Zhu,[6] S. C. Zugravel,[57] and N. Zurlo[135,56]

(ALICE Collaboration)

[1]*A.I. Alikhanyan National Science Laboratory (Yerevan Physics Institute) Foundation, Yerevan, Armenia*
[2]*AGH University of Krakow, Cracow, Poland*
[3]*Bogolyubov Institute for Theoretical Physics, National Academy of Sciences of Ukraine, Kiev, Ukraine*
[4]*Bose Institute, Department of Physics and Centre for Astroparticle Physics and Space Science (CAPSS), Kolkata, India*
[5]*California Polytechnic State University, San Luis Obispo, California, USA*
[6]*Central China Normal University, Wuhan, China*
[7]*Centro de Aplicaciones Tecnológicas y Desarrollo Nuclear (CEADEN), Havana, Cuba*

[8]*Centro de Investigación y de Estudios Avanzados (CINVESTAV), Mexico City and Mérida, Mexico*
[9]*Chicago State University, Chicago, Illinois, USA*
[10]*China Institute of Atomic Energy, Beijing, China*
[11]*China University of Geosciences, Wuhan, China*
[12]*Chungbuk National University, Cheongju, Republic of Korea*
[13]*Comenius University Bratislava, Faculty of Mathematics, Physics and Informatics, Bratislava, Slovak Republic*
[14]*COMSATS University Islamabad, Islamabad, Pakistan*
[15]*Creighton University, Omaha, Nebraska, USA*
[16]*Department of Physics, Aligarh Muslim University, Aligarh, India*
[17]*Department of Physics, Pusan National University, Pusan, Republic of Korea*
[18]*Department of Physics, Sejong University, Seoul, Republic of Korea*
[19]*Department of Physics, University of California, Berkeley, California, USA*
[20]*Department of Physics, University of Oslo, Oslo, Norway*
[21]*Department of Physics and Technology, University of Bergen, Bergen, Norway*
[22]*Dipartimento di Fisica, Università di Pavia, Pavia, Italy*
[23]*Dipartimento di Fisica dell'Università and Sezione INFN, Cagliari, Italy*
[24]*Dipartimento di Fisica dell'Università and Sezione INFN, Trieste, Italy*
[25]*Dipartimento di Fisica dell'Università and Sezione INFN, Turin, Italy*
[26]*Dipartimento di Fisica e Astronomia dell'Università and Sezione INFN, Bologna, Italy*
[27]*Dipartimento di Fisica e Astronomia dell'Università and Sezione INFN, Catania, Italy*
[28]*Dipartimento di Fisica e Astronomia dell'Università and Sezione INFN, Padova, Italy*
[29]*Dipartimento di Fisica 'E.R. Caianiello' dell'Università and Gruppo Collegato INFN, Salerno, Italy*
[30]*Dipartimento DISAT del Politecnico and Sezione INFN, Turin, Italy*
[31]*Dipartimento di Scienze MIFT, Università di Messina, Messina, Italy*
[32]*Dipartimento Interateneo di Fisica 'M. Merlin' and Sezione INFN, Bari, Italy*
[33]*European Organization for Nuclear Research (CERN), Geneva, Switzerland*
[34]*Faculty of Electrical Engineering, Mechanical Engineering and Naval Architecture, University of Split, Split, Croatia*
[35]*Faculty of Engineering and Science, Western Norway University of Applied Sciences, Bergen, Norway*
[36]*Faculty of Nuclear Sciences and Physical Engineering, Czech Technical University in Prague, Prague, Czech Republic*
[37]*Faculty of Physics, Sofia University, Sofia, Bulgaria*
[38]*Faculty of Science, P.J. Šafárik University, Košice, Slovak Republic*
[39]*Frankfurt Institute for Advanced Studies, Johann Wolfgang Goethe-Universität Frankfurt, Frankfurt, Germany*
[40]*Fudan University, Shanghai, China*
[41]*Gangneung-Wonju National University, Gangneung, Republic of Korea*
[42]*Gauhati University, Department of Physics, Guwahati, India*
[43]*Helmholtz-Institut für Strahlen- und Kernphysik, Rheinische Friedrich-Wilhelms-Universität Bonn, Bonn, Germany*
[44]*Helsinki Institute of Physics (HIP), Helsinki, Finland*
[45]*High Energy Physics Group, Universidad Autónoma de Puebla, Puebla, Mexico*
[46]*Horia Hulubei National Institute of Physics and Nuclear Engineering, Bucharest, Romania*
[47]*HUN-REN Wigner Research Centre for Physics, Budapest, Hungary*
[48]*Indian Institute of Technology Bombay (IIT), Mumbai, India*
[49]*Indian Institute of Technology Indore, Indore, India*
[50]*INFN, Laboratori Nazionali di Frascati, Frascati, Italy*
[51]*INFN, Sezione di Bari, Bari, Italy*
[52]*INFN, Sezione di Bologna, Bologna, Italy*
[53]*INFN, Sezione di Cagliari, Cagliari, Italy*
[54]*INFN, Sezione di Catania, Catania, Italy*
[55]*INFN, Sezione di Padova, Padova, Italy*
[56]*INFN, Sezione di Pavia, Pavia, Italy*
[57]*INFN, Sezione di Torino, Turin, Italy*
[58]*INFN, Sezione di Trieste, Trieste, Italy*
[59]*Inha University, Incheon, Republic of Korea*
[60]*Institute for Gravitational and Subatomic Physics (GRASP), Utrecht University/Nikhef, Utrecht, Netherlands*
[61]*Institute of Experimental Physics, Slovak Academy of Sciences, Košice, Slovak Republic*
[62]*Institute of Physics, Homi Bhabha National Institute, Bhubaneswar, India*
[63]*Institute of Physics of the Czech Academy of Sciences, Prague, Czech Republic*
[64]*Institute of Space Science (ISS), Bucharest, Romania*
[65]*Institut für Kernphysik, Johann Wolfgang Goethe-Universität Frankfurt, Frankfurt, Germany*
[66]*Instituto de Ciencias Nucleares, Universidad Nacional Autónoma de México, Mexico City, Mexico*

[67]*Instituto de Física, Universidade Federal do Rio Grande do Sul (UFRGS), Porto Alegre, Brazil*
[68]*Instituto de Física, Universidad Nacional Autónoma de México, Mexico City, Mexico*
[69]*iThemba LABS, National Research Foundation, Somerset West, South Africa*
[70]*Jeonbuk National University, Jeonju, Republic of Korea*
[71]*Johann-Wolfgang-Goethe Universität Frankfurt Institut für Informatik, Fachbereich Informatik und Mathematik, Frankfurt, Germany*
[72]*Korea Institute of Science and Technology Information, Daejeon, Republic of Korea*
[73]*KTO Karatay University, Konya, Turkey*
[74]*Laboratoire de Physique Subatomique et de Cosmologie, Université Grenoble-Alpes, CNRS-IN2P3, Grenoble, France*
[75]*Lawrence Berkeley National Laboratory, Berkeley, California, USA*
[76]*Lund University Department of Physics, Division of Particle Physics, Lund, Sweden*
[77]*Nagasaki Institute of Applied Science, Nagasaki, Japan*
[78]*Nara Women's University (NWU), Nara, Japan*
[79]*National and Kapodistrian University of Athens, School of Science, Department of Physics, Athens, Greece*
[80]*National Centre for Nuclear Research, Warsaw, Poland*
[81]*National Institute of Science Education and Research, Homi Bhabha National Institute, Jatni, India*
[82]*National Nuclear Research Center, Baku, Azerbaijan*
[83]*National Research and Innovation Agency - BRIN, Jakarta, Indonesia*
[84]*Niels Bohr Institute, University of Copenhagen, Copenhagen, Denmark*
[85]*Nikhef, National Institute for Subatomic Physics, Amsterdam, Netherlands*
[86]*Nuclear Physics Group, STFC Daresbury Laboratory, Daresbury, United Kingdom*
[87]*Nuclear Physics Institute of the Czech Academy of Sciences, Husinec-Řež, Czech Republic*
[88]*Oak Ridge National Laboratory, Oak Ridge, Tennessee, USA*
[89]*Ohio State University, Columbus, Ohio, USA*
[90]*Physics Department, Faculty of Science, University of Zagreb, Zagreb, Croatia*
[91]*Physics Department, Panjab University, Chandigarh, India*
[92]*Physics Department, University of Jammu, Jammu, India*
[93]*Physics Program and International Institute for Sustainability with Knotted Chiral Meta Matter (SKCM2), Hiroshima University, Hiroshima, Japan*
[94]*Physikalisches Institut, Eberhard-Karls-Universität Tübingen, Tübingen, Germany*
[95]*Physikalisches Institut, Ruprecht-Karls-Universität Heidelberg, Heidelberg, Germany*
[96]*Physik Department, Technische Universität München, Munich, Germany*
[97]*Politecnico di Bari and Sezione INFN, Bari, Italy*
[98]*Research Division and ExtreMe Matter Institute EMMI, GSI Helmholtzzentrum für Schwerionenforschung GmbH, Darmstadt, Germany*
[99]*Saga University, Saga, Japan*
[100]*Saha Institute of Nuclear Physics, Homi Bhabha National Institute, Kolkata, India*
[101]*School of Physics and Astronomy, University of Birmingham, Birmingham, United Kingdom*
[102]*Sección Física, Departamento de Ciencias, Pontificia Universidad Católica del Perú, Lima, Peru*
[103]*Stefan Meyer Institut für Subatomare Physik (SMI), Vienna, Austria*
[104]*SUBATECH, IMT Atlantique, Nantes Université, CNRS-IN2P3, Nantes, France*
[105]*Sungkyunkwan University, Suwon City, Republic of Korea*
[106]*Suranaree University of Technology, Nakhon Ratchasima, Thailand*
[107]*Technical University of Košice, Košice, Slovak Republic*
[108]*The Henryk Niewodniczanski Institute of Nuclear Physics, Polish Academy of Sciences, Cracow, Poland*
[109]*The University of Texas at Austin, Austin, Texas, USA*
[110]*Universidad Autónoma de Sinaloa, Culiacán, Mexico*
[111]*Universidade de São Paulo (USP), São Paulo, Brazil*
[112]*Universidade Estadual de Campinas (UNICAMP), Campinas, Brazil*
[113]*Universidade Federal do ABC, Santo Andre, Brazil*
[114]*Universitatea Nationala de Stiinta si Tehnologie Politehnica Bucuresti, Bucharest, Romania*
[115]*University of Cape Town, Cape Town, South Africa*
[116]*University of Derby, Derby, United Kingdom*
[117]*University of Houston, Houston, Texas, USA*
[118]*University of Jyväskylä, Jyväskylä, Finland*
[119]*University of Kansas, Lawrence, Kansas, USA*
[120]*University of Liverpool, Liverpool, United Kingdom*
[121]*University of Science and Technology of China, Hefei, China*
[122]*University of South-Eastern Norway, Kongsberg, Norway*
[123]*University of Tennessee, Knoxville, Tennessee, USA*
[124]*University of the Witwatersrand, Johannesburg, South Africa*

[125]*University of Tokyo, Tokyo, Japan*
[126]*University of Tsukuba, Tsukuba, Japan*
[127]*Universität Münster, Institut für Kernphysik, Münster, Germany*
[128]*Université Clermont Auvergne, CNRS/IN2P3, LPC, Clermont-Ferrand, France*
[129]*Université de Lyon, CNRS/IN2P3, Institut de Physique des 2 Infinis de Lyon, Lyon, France*
[130]*Université de Strasbourg, CNRS, IPHC UMR 7178, F-67000 Strasbourg, France, Strasbourg, France*
[131]*Université Paris-Saclay, Centre d'Etudes de Saclay (CEA), IRFU, Départment de Physique Nucléaire (DPhN), Saclay, France*
[132]*Université Paris-Saclay, CNRS/IN2P3, IJCLab, Orsay, France*
[133]*Università degli Studi di Foggia, Foggia, Italy*
[134]*Università del Piemonte Orientale, Vercelli, Italy*
[135]*Università di Brescia, Brescia, Italy*
[136]*Variable Energy Cyclotron Centre, Homi Bhabha National Institute, Kolkata, India*
[137]*Warsaw University of Technology, Warsaw, Poland*
[138]*Wayne State University, Detroit, Michigan, USA*
[139]*Yale University, New Haven, Connecticut, USA*
[140]*Yonsei University, Seoul, Republic of Korea*
[141]*Zentrum für Technologie und Transfer (ZTT), Worms, Germany*
[142]*Affiliated with an institute covered by a cooperation agreement with CERN*
[143]*Affiliated with an international laboratory covered by a cooperation agreement with CERN*

[*]Also at: Max-Planck-Institut fur Physik, Munich, Germany.
[†]Also at: Italian National Agency for New Technologies, Energy, Sustainable Economic Development (ENEA), Bologna, Italy.
[‡]Also at: Dipartimento DET del Politecnico di Torino, Turin, Italy.
[§]Deceased; Also at: An institution covered by a cooperation agreement with CERN.
[‖]Also at: Department of Applied Physics, Aligarh Muslim University, Aligarh, India.
[¶]Also at: Institute of Theoretical Physics, University of Wroclaw, Poland.